



The effect of temperature and material on mains pipe breaks in Gothenburg

Master of Science Thesis in the Master's Programme in Geo and Water Engineering

VALERIA MILONE

Department of Civil and Environmental Engineering
Division of Water Environment Technology

CHALMERS UNIVERSITY OF TECHNOLOGY
Gothenburg, Sweden, 2011
Master's Thesis 2012:160

MASTER'S THESIS 2012:160

The effect of temperature and material on mains pipe breaks in Gothenburg

Master of Science Thesis in the Master's Programme in Geo and Water Engineering

VALERIA MILONE

Department of Civil and Environmental Engineering
Division of Water Environment Technology
CHALMERS UNIVERSITY OF TECHNOLOGY
Gothenburg, Sweden

The effect of temperature and material on mains pipe breaks in Gothenburg

Master of Science Thesis in the Master's Programme in Geo and Water Engineering
VALERIA MILONE

© VALERIA MILONE

Master Thesis2012:160
Department of Civil and Environmental Engineering
Division of Water Environment Engineering
Chalmers University of Technology
SE-412 96 Gothenburg
Sweden
Telephone: + 46 (0)31-772 1000

Cover:
Circumferential pipe break in Avesta municipality, Sweden

Reproservice / Department of Civil and Environmental Engineering Gothenburg,
Sweden

ABSTRACT

One of the most important actions we can take to guarantee a good water supply is to carry out research into how to reduce the amount of water lost in the distribution network. If we can identify and put in place measures to do this, we may be able to achieve substantial savings in resources.

In addition, understanding the mechanisms that cause the network to fail or deteriorate is fundamental to infrastructure management. If a water supply is exposed to aggressive and harmful environmental conditions, this may lead to significant problems.

Despite the fact that Gothenburg has a good water supply system and distribution network, around 17% of the drinking water produced is lost. A large number of breaks occur in the distribution network during the winter. In order to understand the break frequency, all breaks that occurred between the 1st of January 2001 and the 31st of May 2009 were analysed. This thesis also looked at the correlation between breaks and temperature and found that there is a correlation; in particular there is a strong negative correlation between circumferential breaks and water temperature.

By analysing the types of breaks and pipe materials, the weakest pipe materials and sizes were identified.

Lastly, a pipe-soil interaction analysis was carried out, to find out which materials and pipe sizes are more likely to break, using different kinds of soil and different sizes of pipe.

Key words: water mains, pipe break, materials, correlation, temperature.

Contents

ABSTRACT	II
CONTENTS	IV
PREFACE	VI
1 INTRODUCTION	8
1.1. Aims	9
2 BACKGROUND	10
2.1 Geographical context	10
2.1.1 Pipeline network of Gothenburg	11
3 THEORY	13
3.1 Pipe breaks	13
3.2 Axial strain	21
3.3 Hoop strain	23
4 RESULTS AND DISCUSSION	27
4.1 Materials and breaks	27
4.2 Temperature and breaks	32
4.2.1 Initial data	32
4.2.2 Results – temperature and breaks	33
4.3 Pipe-soil interaction	39
4.3.1 Sensitivity analysis	43
5 FURTHER DATA	49
5.1 Considerations on melting snow	50
6 CONCLUSIONS	52
7 REFERENCES	53
8 APPENDIX	55

Preface

This work have been carried out from January 2010 to August 2010 at the Department of Water Environmental Technology, Chalmers University of Technology, Sweden, under the supervision of Prof. Greg Morrison, to whom, first of all, I have to say thank you for welcoming me into his Department. The last part was carried out until December 2010 in Florence, at my home University.

All the data analysed comes from Gothenburg Water and I gratefully acknowledge my advisor Eng. Annika Malm, who followed me during my work and who always encouraged me.

I want to thank my supervisor Prof. Giorgio Federici, who has taught me more than just an exam subject during these years and also Prof. Giovanni Vannucchi.

Last but not least, I need to acknowledge all those who have supported me: my family, firstly, and my closest friends, both the old ones and the newly discovered ones.

Florence, December 2010

Valeria Milone

1 Introduction

In the world, the natural renewable resource fresh water remains fairly constant over the year. Furthermore, the supply sources are well known and mainly exploited, which makes it hard to find a solution to water shortages. A possible way forward would be to decrease the use and the amount of water that is wasted, in particular the high volumes lost due to pipe leaks. Even in countries that do not suffer from water shortages, it would be reasonable to decrease the amount of water wasted. Due to the reasons stated above, one of the most important actions we can take to guarantee a good water supply is to carry out research into how to reduce the amount of water lost in the distribution network. If we can identify and put in place measures to minimize the losses, we may be able to achieve substantial savings in resources.

Moreover, both the search for network losses and the to reduce them have consequences in several areas: on the one hand, there is a social aspect, as less leakage will lead to fewer customer complaints, on the other hand, there are economic benefits through savings in energy and reduced costs for processing and managing water. It is also important to take into account the environmental impact.

Leakages are not easy to find. It is possible to determine the amount of water lost by calculating the difference between the input and output of water in the system, however networks are long and many leaks are not detected. Leakage is defined as ‘not located losses’, and a water leak is defined as ‘a leakage that is found and can be repaired’. Moreover there are pipe breaks; these occur when a pipe is broken. For financial reasons, it is important to water utility providers to minimize leakage and prevent pipe breaks. Another positive effect of this is that the network will be well supplied and that water can be reliably provided to the consumers.

Understanding the mechanisms that cause the network to fail or deteriorate is fundamental to infrastructure management. If a water supply is exposed to aggressive and harmful environmental conditions, this may lead to significant problems. Another interesting question is whether breaks happen because the material loses its properties or because of an increase in the stresses it is subjected to.

Every water leak and pipe break is a health risk. The last few decades have been characterized by an increase in outbreaks of waterborne diseases [2]. A phenomenon that occurred also in highly developed countries. Possible causes of this situation are [18]:

- Faecal contamination of source waters;
- Deficient disinfection;
- Inadequate treatment and distribution under “normal” conditions;
- Intrusion of soil bacteria and wastewater into distribution system networks.

Of the above points, we will focus on the last one. Normally, a distribution network is pressurized. As long as the pressure on the inside of a water pipe is higher than the pressure on the outside, there is no intrusion of water into the pipe. There are occasions when the pressure is approximately equal on the inside and outside, or when the pressure is lower on the inside. This happens in the following situations:

- during the repair of a pipeline resulting in a need to shut off the pipe;
- during the replacement of a part of the system resulting in a need to shut off the pipe;
- in situations when the pressure falls in the network, for example due to power failures in the pumping station or sudden closure of a valve;
- large instantaneous consumption, such as fire water extraction;
- when there is a large leak in a pipe and water is flooding out, the network loses pressure until the affected pipe is turned off, most likely to occur in high located areas
- during flushing or cleaning of a pipe.

Most of the actions normally used to restore network functionality can affect the water quality negatively. Repairs to mains and pipes seem to be a particularly vulnerable act that often puts consumer health at risk. Based on the study by Kirmeyer et al. [7] and on the assertions from the National Academics' Water Science and Technology Board [10], water mains are the most common entrance way used by pathogens [2]. Additionally, some studies have observed experimentally that there is a high risk of pathogen survival when pipes break and are repaired [2]. Nygård et al.'s study gives a further contribution, proving that breaks and maintenance works in the water distribution system cause an increased risk of gastrointestinal illness [11].

1.1. Aims

This work derives from the necessity to investigate the large number of breaks that occur in Gothenburg's network during the winter.

It wants to understand:

- whether a correlation exists between breaks and low temperatures;
- which materials are most subjected to failure;
- which type of break is most frequent;
- what the mechanism of failure is;
- why breaks happen, whether this is because of stress increases or because the material is weakened.

This thesis is divided into three parts: the first part looks at the connection between types of breaks and pipe materials; in the second part, the correlation between the temperature and the pipe breaks in Gothenburg is studied. In the last part, pipe-soil interaction is analysed, to identify which materials and pipe sizes were more subjected to breaks, using different kinds of soil and different sizes of pipe.

2 Background

The risk of pipe breaks in a drinking water system can depend on a variety of factors. Many of these are difficult to detect and some are impossible to prevent. The factors that may cause failures include [1]:

- environment of the pipe (climate, geo-hydrology, geology);
- construction work (pipe bed, fill up under pipe);
- type of pipe (material, diameter, age);
- hydraulics (flow, pressure).

It is common knowledge among those involved in the management of water distribution systems that winter brings about an increase in maintenance activities. This phenomenon is obviously more noticeable in systems located at northern latitudes. There are several studies into the correlation between breaks and low temperatures, especially by the Institute for Research in Construction of National Research Council of Canada ([13], [14]) and by the American Water Works Association ([15], [17]).

Several studies have looked at different types of breaks and the interaction between soil and pipe. In 1996, Rajani et al. [14] developed a mechanical model to calculate stresses on a jointed buried pipe, based on the hypothesis of Winkler, i.e. elastic soil, which takes into account the findings about the impact of temperature on the strengths and the strains. Rajani and Tesfamariam [13] followed this with a more comprehensive formulation, which also takes into account traffic and frost loads. They also looked at the flexural or bending deformations in the longitudinal direction, assuming that soil is an elasto-plastic medium.

The data available to study the water distribution network in Gothenburg is not detailed enough to carry out a precise investigation according to the more comprehensive formulation. For this reason, we decided to follow the methodology of Rajani's first study [14], partly motivated by the fact that the second report was developed based on the findings from the first study.

2.1 Geographical context

When it comes to water availability, Sweden can be defined as a rich country. In fact, Sweden is characterized by almost 100,000 lakes, accounting for 9% of the total area of the country. Moreover, the average river runoff amounts to approximately 200km³ per year. Only 0.5% of the fresh water that is theoretically available is extracted for municipal use. Industry and farmers use approximately three times as much water as the municipal sector. Generally, the water supply and sanitation (including storm water management) are managed and administrated by the local government or municipality administration. The municipality usually owns the facilities and is responsible for the operation. In Sweden there are around 2,000 publically owned treatment plants, of which 200 use surface water [8]. Against this background, it is possible to evaluate more in depth the drinking water distribution system of Gothenburg.

Gothenburg is located on the south-western coast and is the second largest city in Sweden. It has 500,000 inhabitants and the most important port in Scandinavia. Gothenburg was founded at the beginning of the 17th century by the Swedish King Gustav Adolf the Second and soon became an important trade centre. The city was built around the Göta River, which, with a mean flow of 575 m³ per second, provides the city with raw water. The system considered in this study is the water supply system for Gothenburg, which includes the Göta River, the Lake Delsjön and the reserve supply from Lake Rådasjön. Two treatment plants produce the city's drinking water and 1,700 km of water network distributes the drinking water to the consumers.

The system is maintained and managed by Gothenburg Water. The water quality is continuously tested at seven monitoring stations located along the river. At these points, properties of the water such as pH, conductivity and turbidity are measured.

Wastewater is collected and transported to the Wastewater Treatment Plant (WTP) of Rya, located on the island of Hisingen. Here, it is analysed and this is also where the sewage from the municipalities of Ale, Härryda, Kungälv, Mölndal and Partille is treated. Mechanical and chemical treatment are undertaken to carefully process the wastewater, which is then discharged into the sea. Gryaab is responsible for the operation and maintenance of the WTP.

2.1.1 Pipeline network of Gothenburg

The materials used for the construction of pipes have changed overtime. Table 1 is an overview of how the materials used in the city of Gothenburg have varied over the years.

Table 1: Years when different materials were used for pipelines

MATERIAL	YEARS
GREY IRON	1890 - 1970
DUCTILE IRON	since 1968
CONCRETE	1948 - 1980
PE (Polyethylene)	since 1960
STEEL	since 1940
PVC (Polyvinyl chloride)	1960-1980

Most of the network was developed in the second half of the 20th century, as shown in Figure 1.

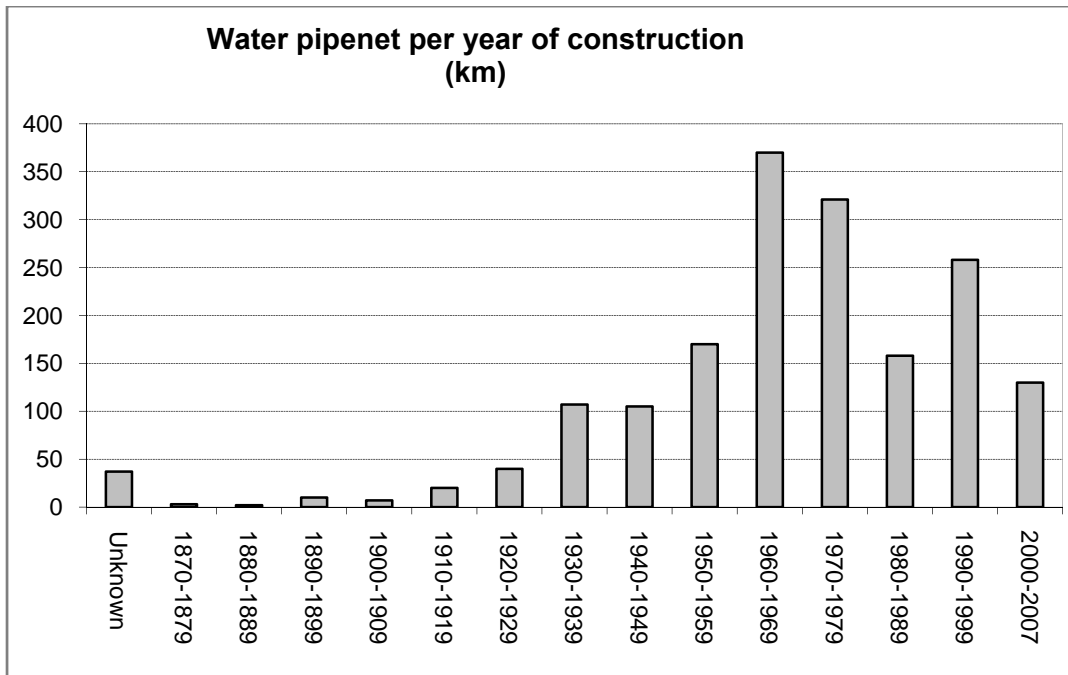


Figure 1: Km of pipeline network divided in decades of construction

The majority of the pipes are made of grey iron, however, this has been gradually replaced by ductile iron and plastic materials since the early 1970s, see Figure 2.

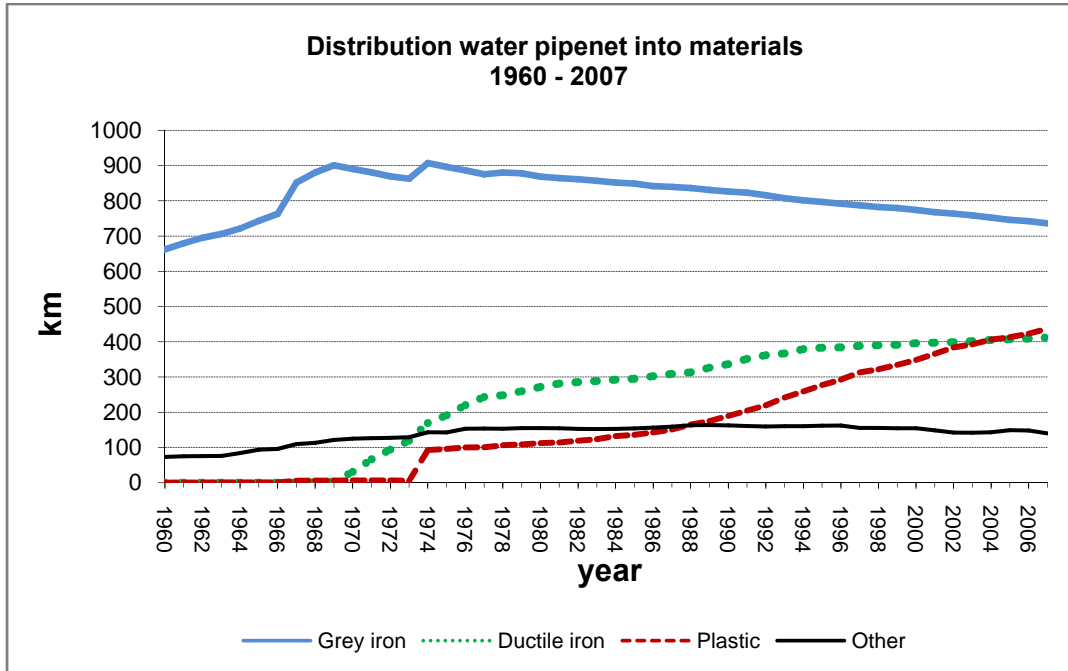


Figure 2: Distribution of water pipeline network divided into materials between 1960 and 2007

3 Theory

3.1 Pipe breaks

Looking at previous studies about this topic ([12], [13], [14]) it was found that the most common types of breaks in pipeline networks are circumferential break, longitudinal break, joint failure and corrosion pit (holes due to corrosion), some of these are shown in Figure 3.



Figure 3: Types of pipe breaks: circumferential (above), corrosion pit (middle), piece out (below). Photos: Gothenburg Water

The typology of failure in the pipeline network is not unique and there are several mechanisms of breaking.

The physical mechanisms that cause pipe rupture are not entirely understood, as they are very complex. In analysis it was found that the physical mechanisms relate mainly to three aspects [12]:

- pipe structural properties, material type, pipe-soil interaction, quality of installation;
- internal loads due to operational pressure and external loads due to soil overburden, traffic loads and third party interference;
- material deterioration due largely to the external and internal chemical, biochemical and electrochemical environment.

In 2006, an analysis method was developed by Tasfamariam et al. [17]. This considers the partial support given by the soil pipe. It takes into account the traffic load and the depth of frozen soil in winter. It also looks at flexion or bending strains and stresses in the longitudinal direction, as the loss of bedding support close to a pipeline puts flexural stresses on the pipe. This is based on the hypothesis of elastic - plastic mediums, rather than on the perfect elastic Winkler's theory. Due to the absence of accurate data about temperatures and soil in Gothenburg, it was decided that this study should follow the first study of Rajani [14], when assessing the behaviour of pipes used in Gothenburg's distribution network. Moreover, the sensitivity analyses conducted in the study from 2004 [13] suggest that if a length of the pipe is unsupported because of a loss of bedding, this has a significant influence on the flexural pipe-soil response, however there is no increase in the stress on the axial pipe-soil response. Thus it is correct to study the soil as an elastic medium since the elasto-plastic influence on the pipe is not very big.

The most common type of break in Gothenburg is circumferential (Table 2, chapter 4.1), so it would be interesting and useful to understand how and why these occur. The breaks are usually caused by longitudinal tensile stress that can be brought by several actions, Figures 4 and 5. One of the possible mechanisms is temperature change, e.g. the difference in temperature between the time when the pipe was positioned and the current temperature: where this is the case, the pipe is subjected to an axial and circumferential strain (contraction if the temperature decreases). Another possible cause is a difference between the external and internal temperature that generates stresses, or bending, on the wall of the pipe.

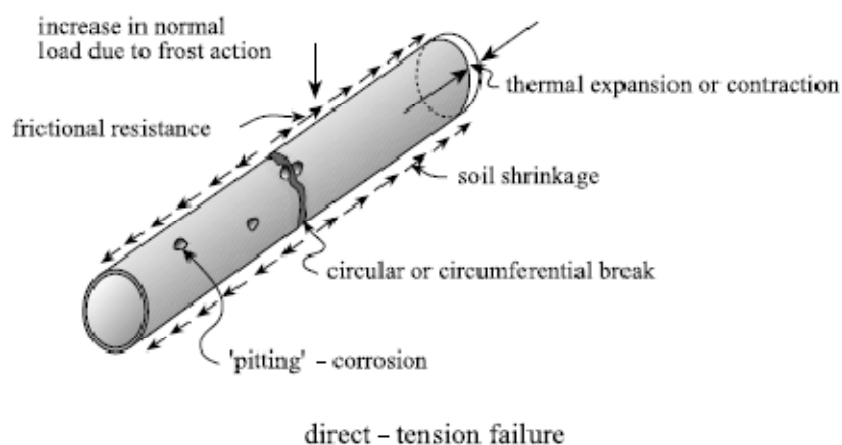


Figure 4: Effects of different loads on a pipe and possible breaks, [12]

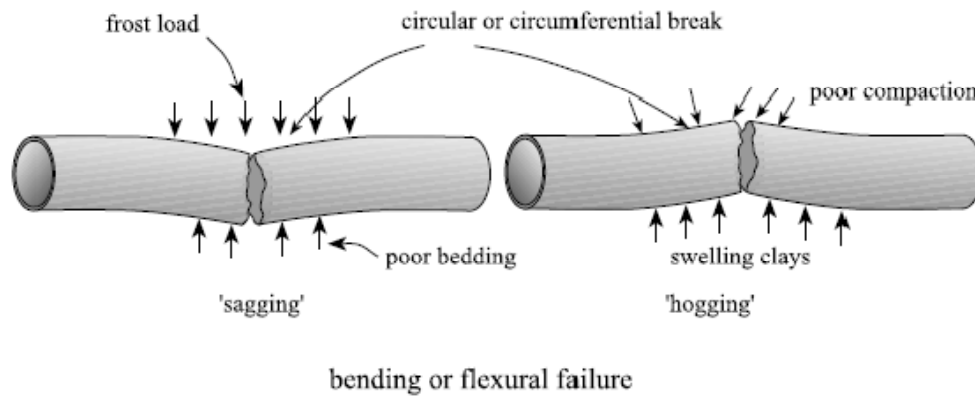


Figure 5: Circumferential break due to bending, [12]

A longitudinal break derives from hoop or circumferential stress, or a bending action in-plane, Figure 6.

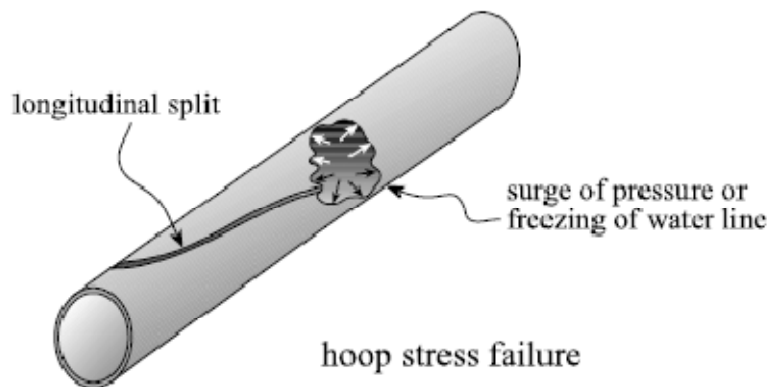


Figure 6: Longitudinal break due to hoop stress, [12]

The longitudinal traction on the pipes can be induced through different mechanisms. If the water network was initially installed at a warm temperature, it will contract (in the axial direction and, to a lesser extent, along the circumference) when the water and ground temperatures decrease. The fact that the network is buried both restrains the deformation of the pipe, due to the pipe-soil interaction (friction), but also leads to a development of axial load. Furthermore, the frictional resistance may increase over time and increase the normal load.

A further increase of tensile stresses in the pipe can be induced by a high content of the clay mineral montmorillonite, which may be subject to material changes in volume in both wet and dry seasonal conditions [3]. Morris [9] reported that the volumetric shrinkage (decrease) in the Texas clay may be in the range 14 - 40%. Flexion (bending) action, due to insufficient bedding support or the swelling of underlying clays, imposes additional longitudinal tensile stresses [14].

The fact that in most of the water system the circumferential cracks occur mainly during the winter suggests that the interaction axial pipe-soil is the principal mechanism. Until now, there is no analytical procedure that explains in a satisfactory manner why extremely cold temperatures lead to an increase in the number of water main breaks.

Recognizing the mechanisms of infrastructure deterioration that lead to breaking is critical to the proactive management of infrastructure assets. If a water supply network is exposed to aggressive and harmful environmental conditions, this can induce significant deterioration and compromise its ability to deliver safe water. Figure 7 shows the "bathtub curve" and describes the lifecycle of a typical buried pipe [13]. It shows the instantaneous probability of failure (hazard function). It is possible to identify three stages in the life of a pipe. The first is called the "burn-in" phase and relates to the period immediately after the installation: here, breaks are usually due to faulty installation or faulty pipes. These interruptions appear gradually and at a declining rate.

In the second phase, the pipe works essentially without problems; there is a low rate of failure caused by random phenomena such as unusually heavy loads and interference of third parties. The final stage is the "wear-out-phase", the last period of the pipe's life, with an increasing failure rate caused by the deterioration and ageing of the pipe.

Not all pipes go through all the three phases, and the length of each phase can vary widely between different pipes and in different conditions.

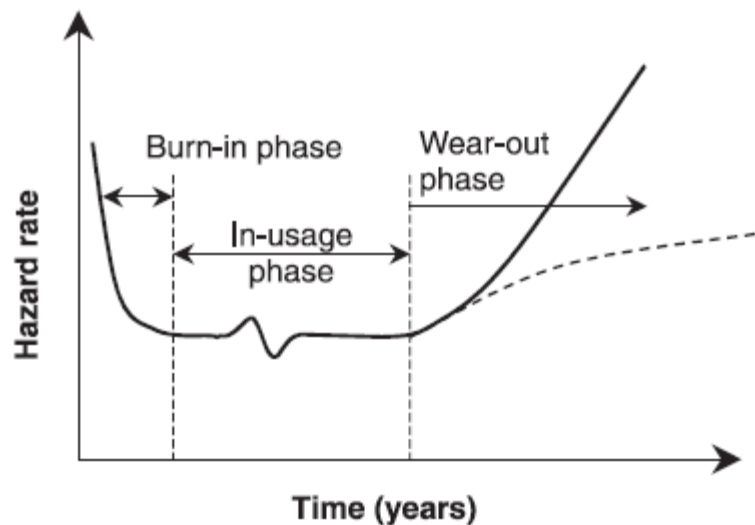


Figure 7: Bathtub curve, [13]

The behaviour of a pipe could also be described by the graph in Figure8. It shows the deterioration in structural reliability, as a safety factor. A Cast Iron (CI) pipe follows the line in the graph and corrosion is the main agent, for Ductile Iron (DI) the main agent is pitting [13].

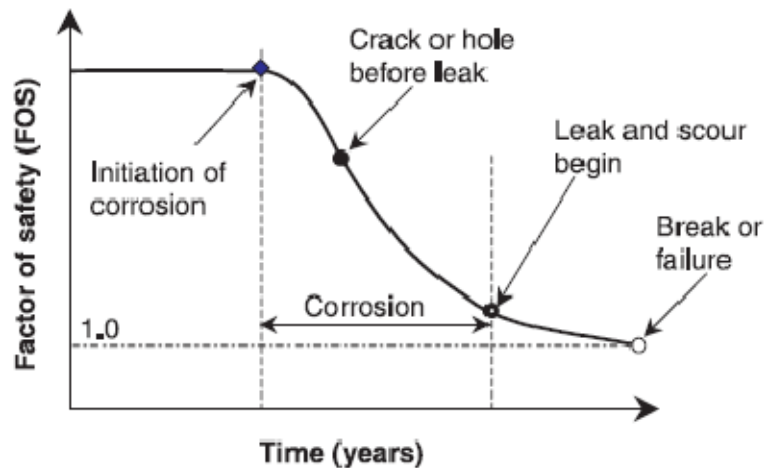


Figure 8: Development of corrosion over time, [13]

The aim of the study is to find the ideal buried pipe for water distribution and the hypotheses of the problem are:

- the pipe deformations are small and always within the elastic range;
- the soil or bedding in the pipe–soil interaction analysis is considered as an elastic Winkler model;
- the stresses at the joints are equal to zero, because it is assumed the pipe is free to move;
- thrust is positive when it results in tensile stresses in the pipe wall and negative when it results in compressive stresses;
- the tensile stresses are positive in the circumferential direction.

To clearly outline the situation, the definitions of the most important concepts are reported and showed in Figure 9:

- *Elasticity*: is the ability of a material to return to its previous shape after the stress is released. In many materials, the relation between applied stress and the resulting strain is directly proportional (up to a certain limit), and a graph representing those two quantities is a straight line (until point 2 in Figure 9).
- *Plasticity* or plastic deformation: is the opposite of elastic deformation and is accepted as unrecoverable strain. Plastic deformation is retained even after the relaxation of the applied stress. Most materials in the linear-elastic category are capable of plastic deformation.
- *Deformation* of the material: is the change in geometry when stress is applied. Deformation is expressed by the displacement field of the material.
- *Strain* or *reduced deformation* is a mathematical term to express the trend of the deformation change among the material field. For uniaxial loading - displacements of a specimen (for example a bar element) is expressed as the quotient of the displacement and the length of the specimen.

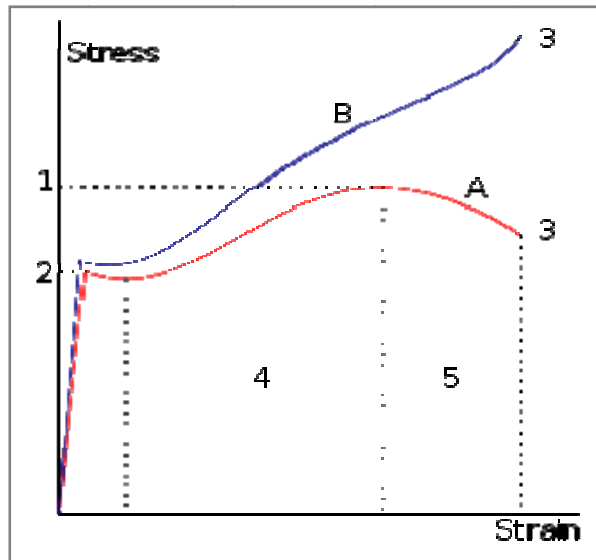


Figure 9: Diagram strain-stress, [12]

Figure 9 shows how the stress develops as the strain increases. It is possible to recognize several different zones and points:

1. Ultimate Strength: is the maximum stress that a material subjected to tension can resist;
2. Yield strength: maximum stress in the elastic area;
3. Rupture;
4. Strain hardening region
5. Necking region.

Line A shows the apparent stress (F/A_0), Line B is the actual (true) stress (F/A), due to the decrease of the section with the strain.

The slope of this line is the Young's Modulus, or the "Modulus of Elasticity." The Modulus of Elasticity can be used to determine stress-strain relationships in the linear-elastic portion of the stress-strain curve. The linear-elastic region is either below the yield point, or if a yield point is not well defined for the material, taken to be between 0 and 0.2% strain, and is defined as the region of strain in which no yielding (permanent deformation) occurs.

Going back up the theory and the hypothesis of the problem it can be observed that there are several defects in the Winkler model, e.g., it assumes no interaction through the soil from location to location and no interaction through shear, nor any volumetric effects. Moreover, the model entails a definition of soil pressure in terms of absolute displacement of the pipe, not the displacement of the pipe relative to the soil. However, considering the uncertainties in modelling pipe-soil interaction, this model is acceptably simple and good enough to permit the analysis of a buried pipe with the consideration of axial effects and radial effects, whilst also taking into account the uncertainty of the data. The circumferential response calculated later on corresponds to that of a rigid pipe but could easily be assumed also in case of a flexible pipe. This consideration is appropriate for the pipe materials (CI and DI) and pipe sizes of interest here.

The axial restraint τ on the pipe is expressed as a function of the normal force acting on the pipe and the frictional characteristics between the surrounding backfill and the pipe material. Usually, the normal force is a result of earth pressure in the vertical direction, but it increases with water pressure and frost penetration (frost loading effects). Thus, the axial restraint τ is expressed by the following relation (equation 1):

where:

(1) $\tau = k_s u$

τ is the axial movement restraint,
 u is the axial displacement,
 k_s is the axial pipe-soil reaction modulus.

k_s depend on the soil and can be defined as indicated by the Committee on Gas and Liquid Pipelines (1984) [4] for sand and clay, or as indicated by Scott [16] from elastic soil (equation 2-4) [21].

Elastic soil (soil as elastic medium)

(2)
$$k_s = \frac{G_s}{4(1 - \nu_s) \frac{D}{2}}$$

G_s is the soil shear modulus,
 D is the external diameter of the pipe,
 ν_s is the soil Poisson's ratio.

Clays

(3)
$$k_s = \frac{\alpha s_u}{u_y}$$

α is the adhesion coefficient,
 s_u is the not drained shear strength of clays,
 u_y is the displacement required to develop ultimate axial resistance (under suggestion of Committee on Gas and Liquid Pipelines, u_y is 2,5-5 mm in loose to dense sands and 5-10 mm in stiff clays).

Sand

(4)
$$k_s = \frac{0.5(\gamma_s H)(1 + K_0) \tan \delta}{u_y}$$

γ_s is the submerged unit weight,
 H is the burial depth of the water mains from surface to the centre line of the pipe,
 K_0 is the coefficient of active resistance at rest,
 δ is the frictional angle between the pipe material and the surrounding backfill.

The equilibrium for a pipe element dx , i.e. the element in the circle in Figure 10, enlarged in Figure 11, is given by the equation (5):

(5) $\frac{\partial P}{\partial x} - S\tau = 0$ where
 P is the axial load in the pipe
 x is the axial coordinate
 S is the external circumference of the pipe
for $u < u_y$ and τ is the axial pipe-soil restraint described in (1)

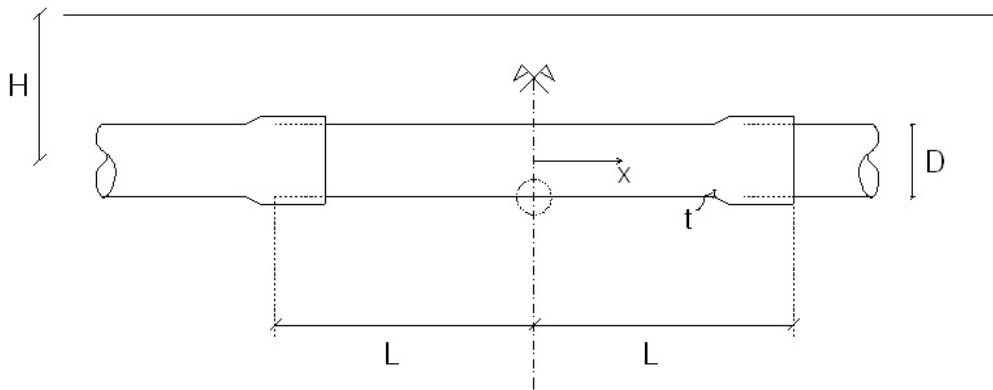


Figure 10: View of a jointed buried pipe

Supposing the pipe to be thin ($S = \pi D$), the axial load can be indicated by axial stress and cross-sectional area as: $P = \sigma_x(\pi Dt)$, where D is the external diameter and t is the wall thickness. Substituting this expression in (5), the equilibrium equation becomes (6):

(6) $\frac{\partial \sigma_x}{\partial x} - \frac{k_s}{t} u = 0$ for $u < u_y$

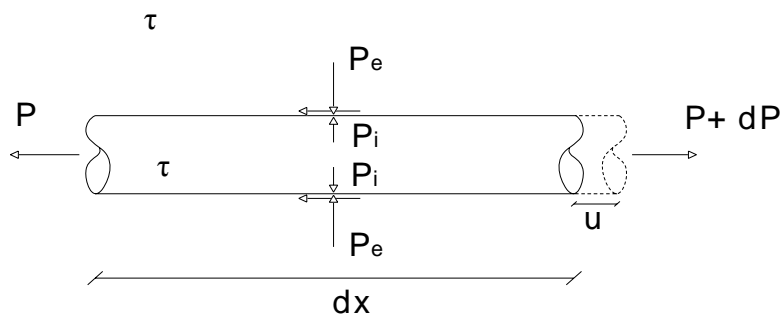


Figure 11: Infinite element of the pipe to be studied

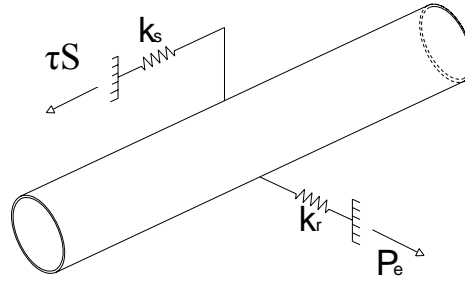


Figure 12: View of the pipe; the soil response is denoted with a spring, as in the Winkler model

3.2 Axial strain

To calculate the axial strain, it is necessary to take into account the effect of the temperature, in addition to water and external pressures.

If the pipe keeps its behaviour at the elastic limit, the total axial strain ε_x is given by:

where:

$$(7) \quad \varepsilon_x = \varepsilon_x^f + \varepsilon_x^w + \varepsilon_x^T$$

ε_x^f corresponds to axial pipe resistance,
 ε_x^w corresponds to water and earth radial pressures,
 ε_x^T corresponds to temperature contraction or dilatation.

Particularly we have:

$$(8) \quad \varepsilon_f = \frac{\sigma_x}{E_p}$$

where:
 E_p is the elastic modulus of the pipe material

The axial strain ε_x^w is given as a combination of hoop stress (“stretching” σ_θ) and radial stress (“pinching” σ_r), due to internal water pressure, P_i , and external radial soil restraint, P_e . Stresses in the axial direction can be expressed as multiply radial and hoop stresses for Poisson’s ratio, ν .

$$(9a) \quad \varepsilon_x^w = -\nu \frac{\sigma_\theta}{E_p} - \nu \frac{\sigma_r}{E_p}$$

or

$$(9b) \quad \varepsilon_x^w = -\nu \frac{D}{t} \frac{(P_i - P_e)}{2E_p} + \nu \frac{(P_i + P_e)}{2E_p}$$

The effect of the temperature alteration is taken into account in the last term and expressed by the equation (10):

$$(10) \quad \varepsilon_x^T = \alpha_p \Delta T \quad \text{where } \alpha_p \text{ is the expansion coefficient of the pipe material.}$$

Replacement of the strain elements given by (8), (9) and (10) in (7) leads to the equation (11):

$$(11) \quad \varepsilon_x = \frac{\sigma_x}{E_p} - \nu \frac{D}{t} \frac{(P_i - P_e)}{2E_p} + \nu \frac{(P_i + P_e)}{2E_p} + \alpha_p \Delta T$$

It is also known that axial strain is the first differentiation of the displacement (11) with respect to the direction, i.e. the differentiation of (11) with respect to x , assuming a constant temperature in the axial direction; this gives:

$$(12) \quad \frac{\partial \sigma_x}{\partial x} = E_p \frac{\partial^2 u}{\partial x^2} + \frac{\nu D}{2t} \left(\frac{\partial P_i}{\partial x} - \frac{\partial P_e}{\partial x} \right) - \frac{\nu}{2} \left(\frac{\partial P_i}{\partial x} + \frac{\partial P_e}{\partial x} \right)$$

The combination of (6) and (12) gives

$$(13) \quad E_p \frac{\partial^2 u}{\partial x^2} + \frac{\nu D}{2t} \left(\frac{\partial P_i}{\partial x} - \frac{\partial P_e}{\partial x} \right) - \frac{\nu}{2} \left(\frac{\partial P_i}{\partial x} + \frac{\partial P_e}{\partial x} \right) - \frac{k_s}{t} u = 0$$

but internal pressure (water pressure) does not usually vary with the x coordinate, consequently

$$\frac{\partial P_i}{\partial x} = 0$$

thus it is possible to write (13) in the following way

$$(14) \quad E_p \frac{\partial^2 u}{\partial x^2} - \frac{\nu}{2} \left(1 + \frac{D}{t} \right) \frac{\partial P_e}{\partial x} - \frac{k_s}{t} u = 0$$

3.3 Hoop strain

Hoop strains can be defined as a combination of axial stress, radial internal and external pressure and temperature variation, as for the axial strain. The formulas below (15) and (16) relate to the hoop strain:

$$(15) \quad \varepsilon_{\theta} = \varepsilon_{\theta}^f + \varepsilon_{\theta}^w + \varepsilon_{\theta}^T$$

$$(16) \quad \varepsilon_{\theta} = -v \frac{\sigma_x}{E_p} + \frac{D}{t} \frac{(P_i - P_e)}{2E_p} + v \frac{(P_i + P_e)}{2E_p} + \alpha_p \Delta T$$

It is also possible to express the hoop strain as a function of the radial displacement, u_r :

$$\varepsilon_{\theta} = \frac{u_r}{\left(\frac{D}{2}\right)}$$

By using formula (11) and substituting in (16), the relation becomes:

$$(17) \quad \frac{u_r}{\left(\frac{D}{2}\right)} = \varepsilon_{\theta} = -v \frac{\partial u}{\partial x} + (1 - v^2) \frac{D}{t} \frac{(P_i - P_e)}{2E_p} + v(1 + v) \frac{(P_i + P_e)}{2E_p} + \alpha_p(1 + v)\Delta T$$

The following relation is also true:

$$u_r = \frac{D}{2} \left[-v \frac{\partial u}{\partial x} + (1 - v^2) \frac{D}{t} \frac{(P_i - P_e)}{2E_p} + v(1 + v) \frac{(P_i + P_e)}{2E_p} + \alpha_p(1 + v)\Delta T \right]$$

For a hole in an infinite medium, the relation between the force and the displacement is given by

$$(18) \quad P_e = k_r u_r = \frac{E_s}{\left(\frac{D}{2}\right) (1 + \nu_s)} u_r$$

which can also be written as follows:

$$u_r = \frac{P_e}{k_r} = \frac{P_e \left(\frac{D}{2}\right) (1 + \nu_s)}{E_s}$$

where k_r is the radial stiffness, E_s is the elastic modulus and ν_s is the Poisson's ratio, all relating to the surrounding soil.

By substituting the radial displacement given by (17) in (18), it is possible to express the external radial pressure P_e as a function of axial pipe strain, internal pressure and temperature change:

$$(19) \quad \beta_1 P_e = \beta_2 P_i - \frac{\nu E_s}{(1 + \nu_s)} \frac{\partial u}{\partial x} + \eta E_p \alpha_p \Delta T$$

or

$$P_e = \frac{1}{\beta_1} \left[\beta_2 P_i - \frac{\nu E_s}{(1 + \nu_s)} \frac{\partial u}{\partial x} + \eta E_p \alpha_p \Delta T \right]$$

where the constants β_1 , β_2 and η are given by:

$$\beta_1 = 1 + \eta(1 - \nu) \frac{D}{2t} - \eta \frac{\nu}{2}$$

$$\beta_2 = \eta(1 - \nu) \frac{D}{2t} + \eta \frac{\nu}{2}$$

$$\eta = \frac{E_s(1 + \nu)}{E_p(1 + \nu_s)}$$

Differentiating (19) with respect to x and substituting it in (14) means that it is possible to express the axial strain ε_x as follows:

$$(20a) \quad \left[E_p + \frac{\nu^2 E_s}{2\beta_1(1 + \nu_s)} \left(1 + \frac{D}{t} \right) \right] \frac{\partial^2 u}{\partial x^2} - \frac{k_s}{t} u = 0$$

$$(20b) \quad \frac{\partial^2 u}{\partial x^2} - \frac{k_s}{\left[E_p + \frac{\nu^2 E_s}{2\beta_1(1 + \nu_s)} \left(1 + \frac{D}{t} \right) \right] t} u = 0$$

The solution to this second-order equation is given in the study of Rajani and is

$$(21) \quad u = C_1 e^{-\gamma x} + C_2 e^{+\gamma x}$$

where γ is a parameter that shows the ratio of soil subgrade and pipe stiffness; the reciprocal of γ is the characteristic length and it is a measure of the elastic interaction between the elastic foundation and the pipe.

$$(22) \quad \gamma^2 = \frac{k_s}{\kappa E_p t} = \frac{k_s}{E_p t \left[1 + \frac{v^2 E_s}{2\beta_1(1+v_s)E_p} \left(1 + \frac{D}{t} \right) \right]}$$

with

$$\kappa = \left[1 + \frac{v^2 E_s}{2\beta_1(1+v^2)E_p} \left(1 + \frac{D}{t} \right) \right]$$

The influence of radial restraint on the axial pipe-soil interaction is represented by k ; when there is no radial restraint $k=1$.

The boundary conditions used to calculate the constants C_1 and C_2 come from the analysis of the problem. Due to symmetry consideration in the mid-span of the pipe the axial movement would be zero (the mid-span is the centre of the axial reference and the whole length of the pipe it is indicated as $2L$), so

$$(23) \quad u(x = 0) = C_1 + C_2 = 0$$

Moreover, the axial stresses at the end of the pipe are zero, because it is allowed to move. Expressing axial stress as

$$(24) \quad \sigma_x = \chi_1 E_p \frac{\partial u}{\partial x} + \chi_2 P_i - \chi_3 E_p \alpha_p \Delta T$$

where

$$\chi_1 = 1 + \frac{v^2}{2(1+v_s)} \frac{E_s}{\beta_1 E_p} \left(1 + \frac{D}{t} \right)$$

$$\chi_2 = \frac{v}{2} \left[\left(1 - \frac{\beta_2}{\beta_1}\right) \frac{D}{t} - \left(1 + \frac{\beta_2}{\beta_1}\right) \right]$$

$$\chi_3 = 1 + \frac{v\eta}{2\beta_1} \left(1 + \frac{D}{t}\right)$$

and considering that $\sigma_x(x = L) = 0$, the constants are solved by:

$$(25) \quad C_1 = -C_2 = \frac{(\chi_2 P_i - \chi_3 \alpha_p E_p \Delta T)}{\chi_1 \gamma E_p (e^{-\gamma L} + e^{+\gamma L})}$$

It is now possible to calculate either the axial strain or the hoop strain from (11) and (16).

The hoop stress for a thin-walled pipe is given by

$$(26) \quad \sigma_\theta = \frac{P_i - P_e}{2} \left(\frac{D}{t}\right)$$

Expressing it in a non-dimensional form, it becomes:

$$(27) \quad \frac{P_i \left(\frac{D}{t}\right)}{\sigma_\theta} = \frac{2}{1 - \frac{P_e}{P_i}} = \mathcal{F} \left\{ \frac{D}{t}, \frac{E_p}{E_s}, v_p, v_s, k_s, K \right\}$$

The radial stress as expressed in (9b) is assumed to vary linearly, while the hoop stress is assumed to be constant across the wall thickness. The validity of these assumptions is ratified by Rajani's study.

These equations all relate to a buried pipe and can be used to carry out a sensitivity analysis to understand how the response to the problem changes as the main influent variables change.

4 Results and discussion

The aim of the first part of the thesis is to analyse the connection between breaks and materials of pipes. The second part wants to understand whether there is any correlation between temperature and pipe breaks in Gothenburg. In the last part, the interaction between pipes and soil is studied, looking firstly at materials and size, secondly at different kinds of soil and different sizes of pipe, in particular because the ratio between the diameter and thickness of the pipes has a strong influence on the behaviour of the pipes.

Analysed data provided by Gothenburg Water:

- Outdoor temperatures from 2001/01/01 till 2009/12/31;
- Drinking water temperatures from 2001/01/01 till 2009/01/31, from Lake Delsjön;
- Pipe breaks from 2001/01/01 till 2009/05/30. All pipe break data where the material and construction year of the broken pipe is known is included.

4.1 Materials and breaks

Several studies confirm that the material more sensitive to low temperatures is iron, particularly grey and ductile iron ([5], [6], [13], [14]). This was confirmed when the breaks that occurred in Gothenburg between 2001 and 2009 were analysed. As seen in Figure 13, the highest frequency of breaks occurs in grey iron pipes.

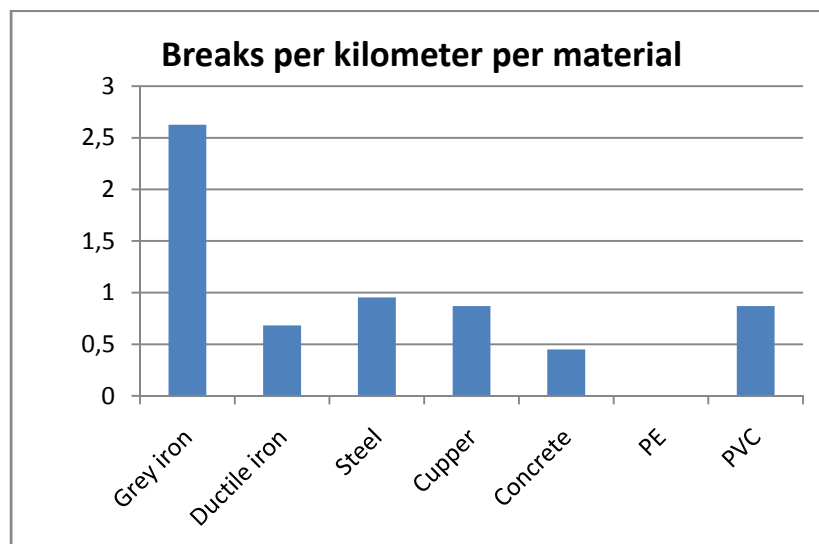


Figure 13: Frequency of breaks divided into material

In this study, we have chosen to look at grey iron and ductile iron, as these are commonly used in the network, and because of the high break frequency of the grey iron.

Due to the impact that the age of the network could have on its functionality, Figure 14 shows the decade of construction of pipelines routes, for both the materials selected.

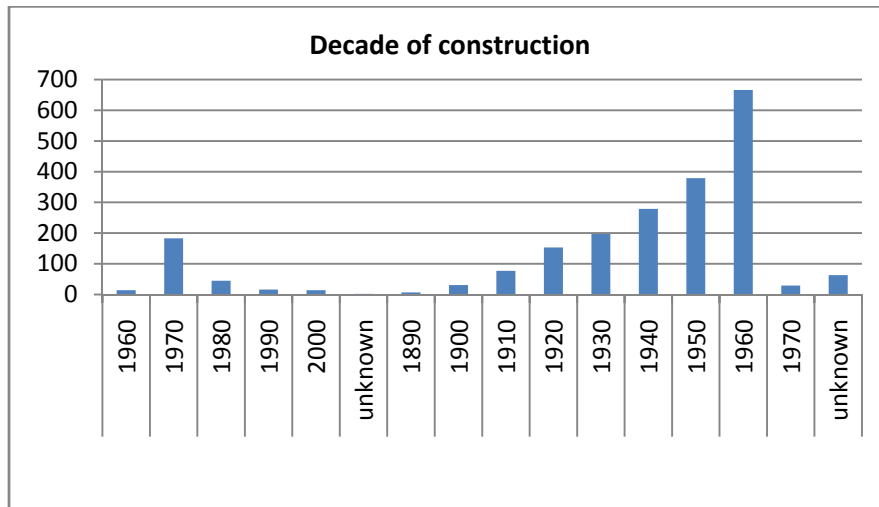


Figure 14: Number of breaks 2001-2009 divided per decade of construction of pipes

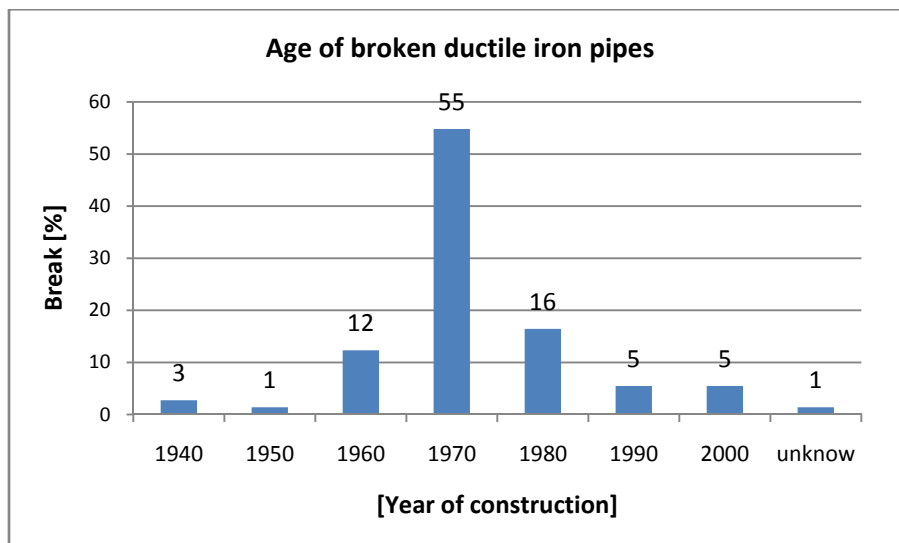


Figure 15: Percentage of breaks divided per decades of construction for ductile iron pipes

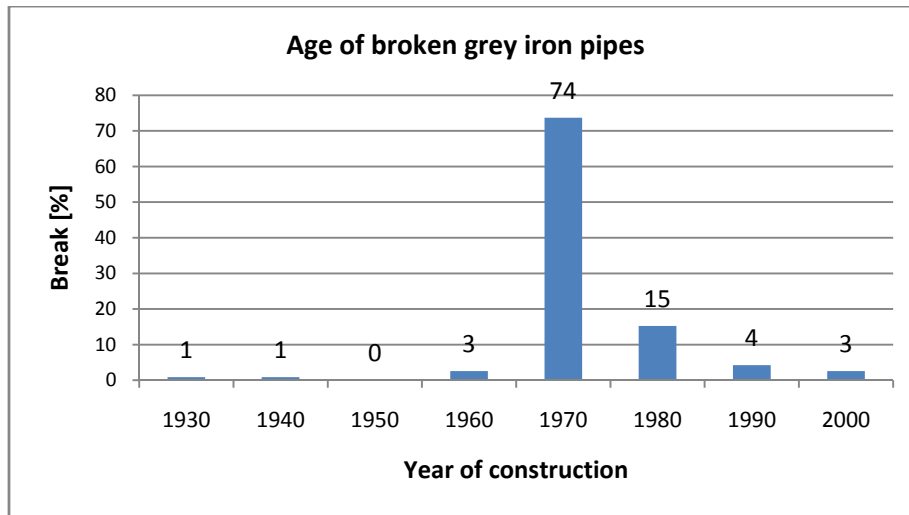


Figure 16: Percentage of breaks divided per decades of construction for grey iron pipes

Another fundamental aspect to understanding the failure mechanism is the type of break. All breaks were divided into seven categories:

- circumferential breaks;
- corrosion pit breaks;
- joint breaks;
- longitudinal breaks;
- piece out of the pipe breaks;
- other breaks (material insufficient, external damage, wrong connection, unclear);
- total breaks.

Table 2: Number of breaks for each category, all materials, 2001-2009

TYPE OF BREAK	ABB.	NUMBER	%
circumferential breaks	C.B.	1185	48
corrosion pit breaks	CP.B.	507	20
joint breaks	J.B.	269	11
longitudinal breaks	L.B.	219	9
piece out of the pipe breaks	PO.B.	156	6
other breaks	O.B.	144	6
total breaks	T.B.	2480	100

Figure 17 shows that for ductile iron the most frequent type of break is corrosion pit, while circumferential breaks are the most common in grey iron, see Figure 18.

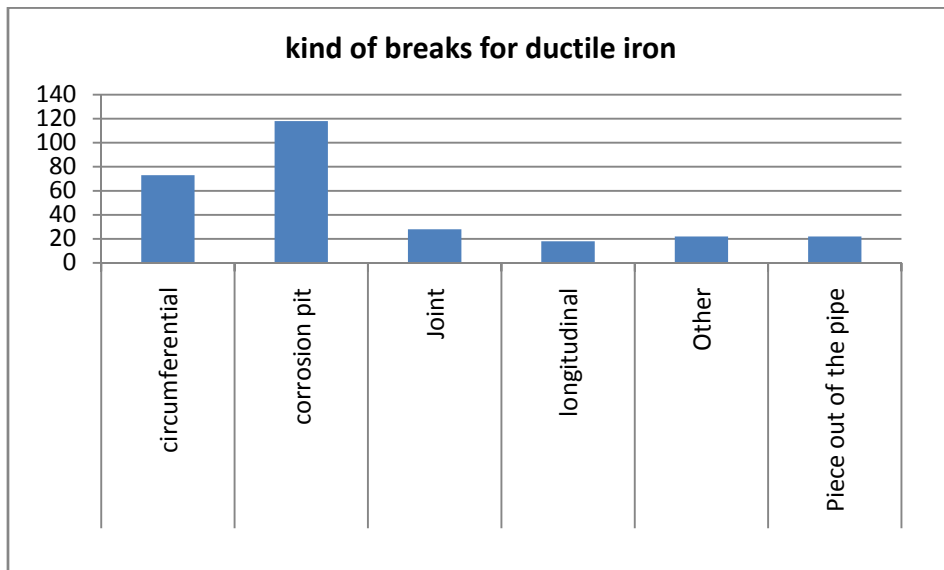


Figure 17: Breaks in ductile iron pipes 2001-2009 divided per type of break

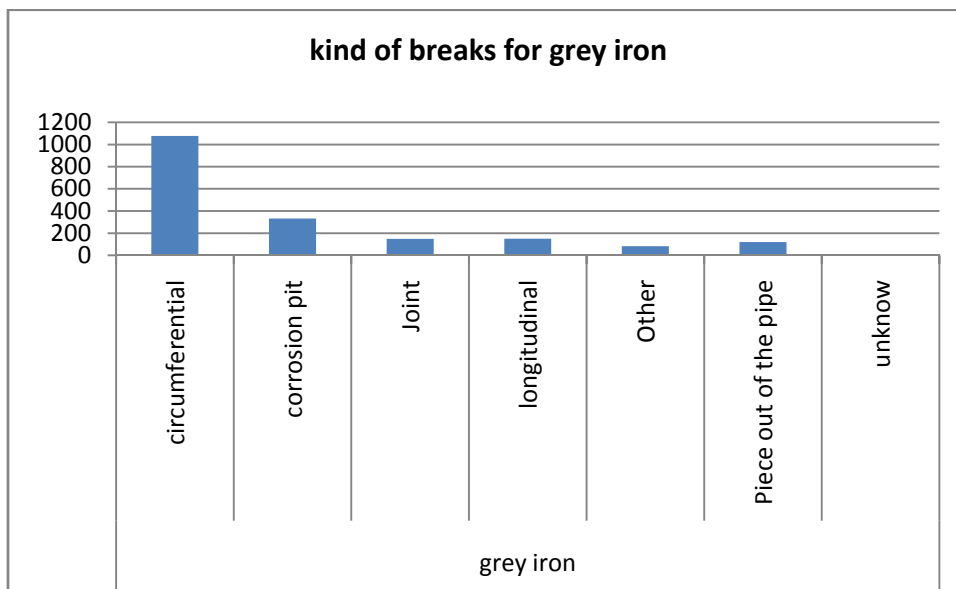


Figure 18: Breaks in grey iron pipes 2001-2009 divided per type of break

Another important fact to remember is that the size of the pipe is a factor influencing the break. Figure 19 and 20 show the number of breaks per km of pipe for ductile iron and grey iron per diameter. They demonstrate that for ductile iron, pipes with a nominal diameter of 200 mm are the most fragile, while the grey iron pipes are more vulnerable at 100 mm diameter.

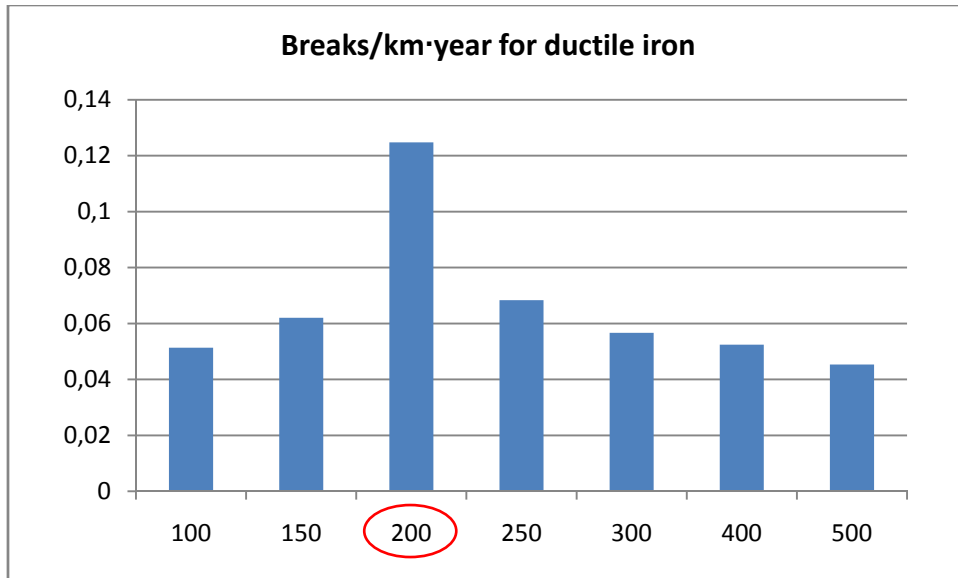


Figure 19: Ductile iron breaks per km, year divided in diameter.

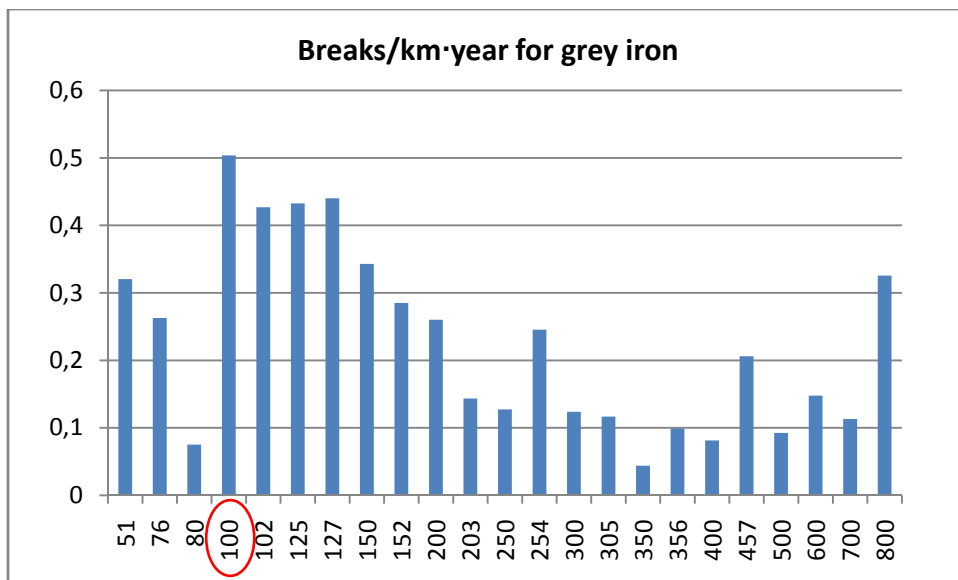


Figure 20: Grey iron breaks per km, year divided in diameter.

4.2 Temperature and breaks

4.2.1 Initial data

There are two kinds of variables in statistics: the first is the continuous variable, which can take on all the values on a continuous scale; the second is the discrete variable, which can assume only determinate values. Breaks are a discrete variable because it is possible to count them and they cannot assume all the values in a range; they are all integers.

Figure 21 shows that the number of breaks increases in the winter time and that it is correct to assume that there is a correlation between temperature and the number of breaks.

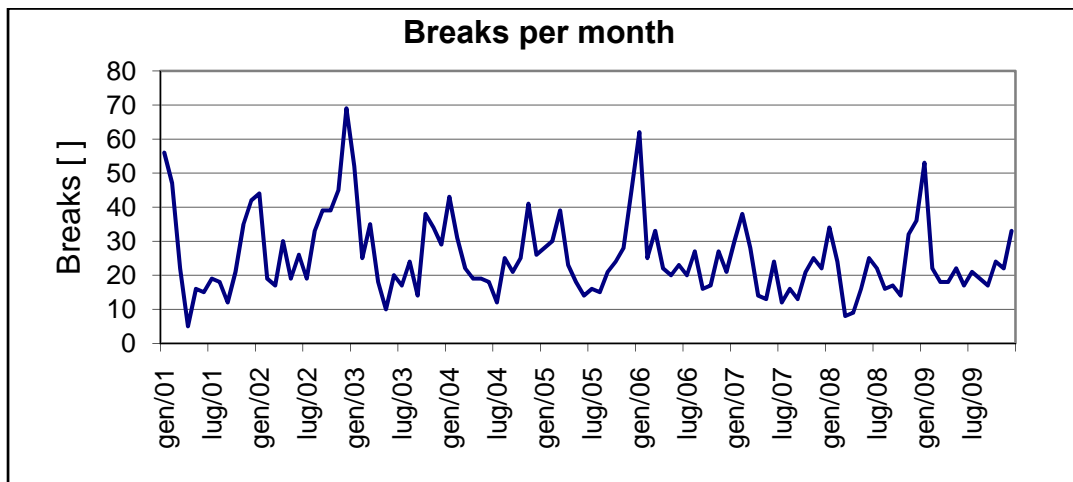


Figure 21: Monthly number of breaks during the period January 2001 until July 2009

Another graph that evidences the high number of breaks during the winter time is shown in Figures 22 and 23. These figures show the cumulative number of breaks over time. The number of breaks is summed up day by day, from the 1st of August 2008 until the 30th of April 2009, and the water temperature is related to the total number of breaks. It is clear that the number of breaks increases rapidly in the winter months, to become almost constant again as the temperature rises in the spring.

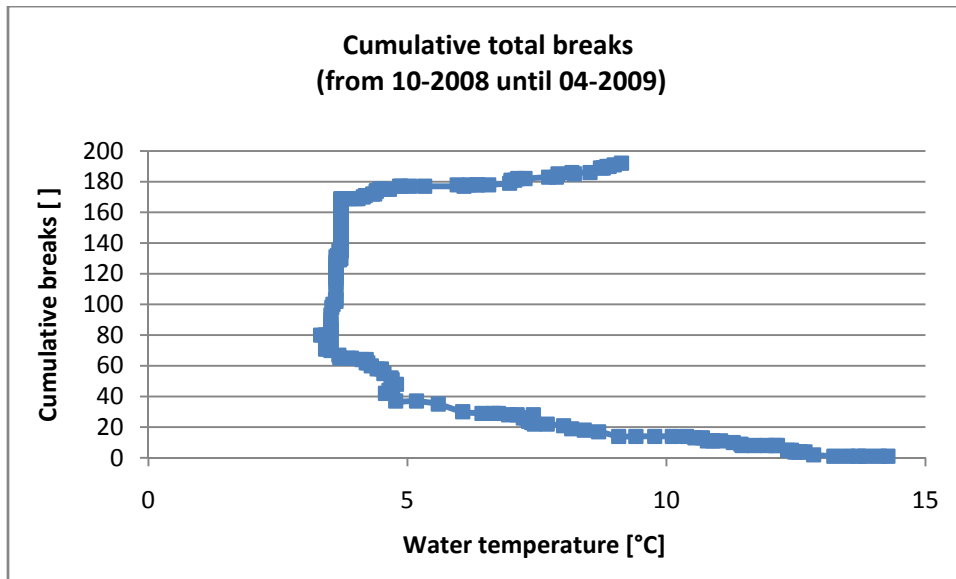


Figure 22: Curve of cumulative breaks

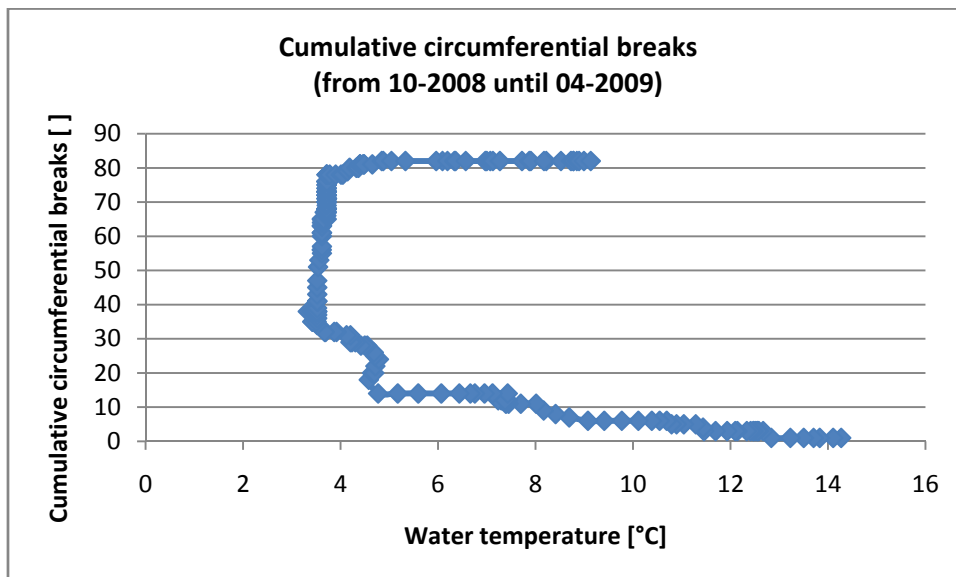


Figure 23: Curve of cumulative circumferential breaks

4.2.2 Results – temperature and breaks

Firstly it was necessary to organize the data. According to Sturges's formula, used to find out how many intervals (C) it is appropriate to divide available data into, the optimal number of classis is:

$C=1+10/3 \log(N)=12,31$, where N is the number of data intervals (here temp degrees)

The detailed results are shown in the Appendix.

Breaks were divided according to type and then aggregated to temperature intervals of 2 degrees. In parallel, the days on which temperatures within the pre-determined intervals were recorded were counted. The latter analysis was conducted for a period of 8 years, from 2001 to 2009.

There are two graphs:

- BREAKS PER DAY: shows how many breaks per day there are in each interval

$$\frac{\#breaks}{\#days}$$

A trend line is inserted to represent the data, but without taking the lowest temperatures into account. This is done because of the strong oscillation that occurred due to the absence of days with the lowest temperatures. To obtain a good and accurate trend line it was necessary to remove the lowest temperatures.

- NORMALIZED BREAKS AND DAYS: shows how many breaks and how many days are recorded at a specific temperature, using the same scale. The sum of the normalized breaks and the sum of the normalized days is 1.

Normalized breaks

Normalized days

$$\frac{\#breaks}{total\ breaks}$$

$$\frac{\#days}{total\ days}$$

both for each temperature interval.

This analysis was carried out in order to compare and identify a possible correlation with the temperature. In fact, it is necessary to know the number of days on which a particular temperature has been recorded. Without this information, you would expect to have a lot of breaks at the most common temperature. Our aim is to determine whether breaks are more likely to occur at a certain temperature simply because a particular temperature was recorded on the majority of the analysed days, or because a correlation exists between the temperature and the likelihood of pipe failure. Furthermore, it is useful to calculate both the total number of breaks (blue line) and the total number of days (red line) for each interval. This is important because it allows us to compare two different kinds and amounts of data using the same scale.

The same analysis was first carried out with respect to air temperature and then with respect to water temperature.

4.2.2.1 Air Temperature [C°]

The first column of Table 3 shows the temperature ranges chosen; the second column shows the number of days with those air temperatures. The remaining columns illustrate the number of breaks at each temperature, for each type of break.

Table 3: Breaks of each type and for each air temperature interval, all materials

TEMP. INTERVAL	NUMBER OF DAYS AT THE SPECIFIED AIR TEMP.	C. B.	CP. B.	J. B.	L. B.	PO. B.	O. B.	T.B.
[-15:-13.01]	4	6	1	0	0	0	0	7
[-13:-11.01]	2	0	0	1	0	0	0	1
[-11:-9.01]	12	16	2	2	0	0	0	20
[-9:-7.01]	17	14	5	5	4	1	2	31
[-7:-5.01]	53	43	11	11	6	4	6	79
[-5:-3.01]	85	57	9	8	4	4	9	94
[-3:-1.01]	166	104	27	28	16	13	5	194
[-1:0.99]	222	147	33	17	22	10	15	249
[1:2.99]	277	174	41	16	25	25	17	308
[3:4.99]	332	179	40	30	14	9	15	293
[5:6.99]	272	111	42	26	14	9	15	225
[7:8.99]	209	62	21	18	13	5	11	131
[9:10.99]	242	56	40	18	15	7	12	151
[11:12.99]	235	42	32	20	11	17	4	128
[13:14.99]	250	48	40	18	14	14	8	148
[15:16.99]	315	53	50	29	21	14	12	180
[17:18.99]	186	37	28	12	15	8	8	112
[19:20.99]	124	10	17	9	16	11	2	76
[21:22.99]	58	15	13	1	7	4	2	44
[23:24.99]	11	3	2	0	2	1	1	9

The data in Table 3 is illustrated in Figures 24 and 25. Figure 24 shows the number of breaks per day for each type of break and for each temperature interval. The trend line is represented by the red curve. The same scale is used in Figure 24b, which instead highlights the number of breaks out of the total number of breaks, in relation to the temperature and to the number of days at that temperature.

Looking at these graphs, it is possible to understand the behaviour of circumferential breaks. These do not follow the trend of the day line (red line Figure 24b) but peak at

low temperatures. This means that there is a correlation between low temperature and circumferential breaks. Moreover, this correlation does not hold for the other types of breaks, as their trend lines follow the day line almost exactly (see Appendix). This confirms that the number of breaks is higher simply because there are more days at which a particular temperature is recorded.

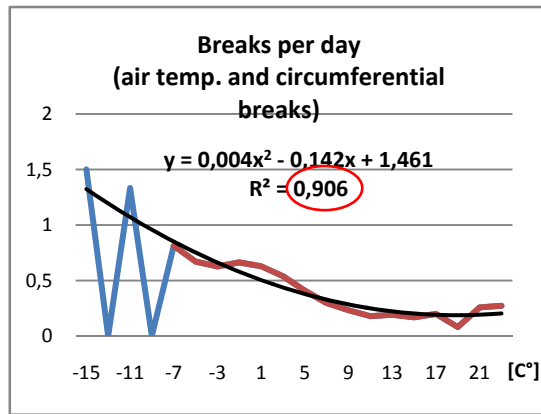


Figure 24a: Daily circumferential breaks with air temperature

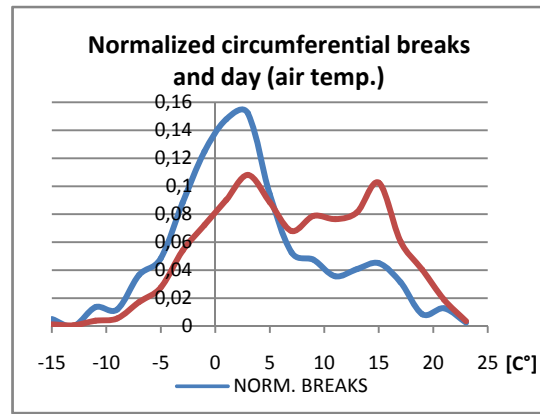


Figure 24b: Normalized circumferential breaks and normalized day with air temperature

There is also a correlation between the total number of breaks and low temperatures, due above all to the fact that almost half of these are circumferential breaks (see Table 2).

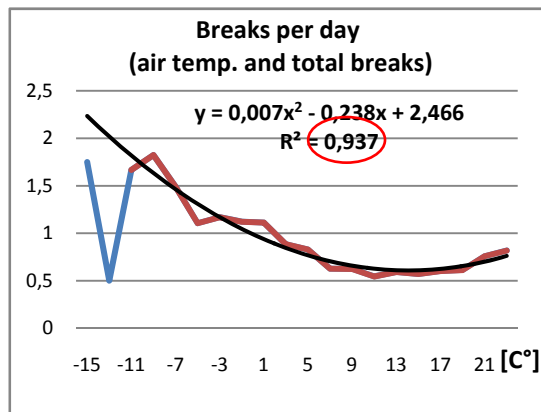


Figure 25a: Daily total breaks with air temperature

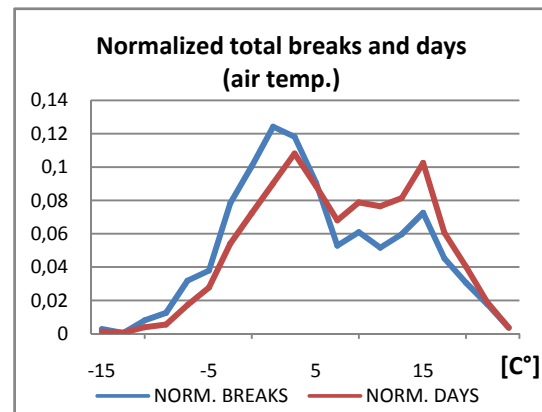


Figure 25b: Normalized total breaks and normalized day with air temperature

4.2.2.2 Water Temperature [C°]

The same methodology which was used to divide and study the data on breaks and air temperature was repeated with water temperature data.

Table 4 shows the results of the division into temperature intervals of two degrees. To be precise, it is necessary to set the first interval to -1°C to 0,99, even though the

water temperature cannot have a negative value. This was necessary to keep the same ranges of values used for the air temperature.

Table 4: Breaks of each type and for each water temperature interval

TEMP INTERVAL	NUMBER OF DAYS AT THE SPECIFIED WATER TEMP.	C. B.	CP. B.	J. B.	L. B.	PO. B.	O. B.	TOT. B.
[-1:0.99]	0	0	0	0	0	0	0	0
[1:2.99]	302	249	45	43	29	14	15	395
[3:4.99]	778	441	116	71	50	46	52	776
[5:6.99]	249	87	40	22	17	8	17	191
[7:8.99]	236	99	45	16	10	6	18	194
[9:10.99]	206	59	33	13	11	7	9	132
[11:12.99]	182	53	38	14	13	10	5	133
[13:14.99]	294	45	48	28	15	17	6	159
[15:16.99]	181	47	28	13	15	6	4	113
[17:18.99]	463	75	77	34	36	30	9	261
[19:20.99]	159	29	34	14	21	9	8	115
[21:22.99]	22	1	3	1	2	3	1	11
[23:24.99]	0	0	0	0	0	0	0	0

As in the previous case, circumferential breaks have the highest correlation with low temperatures, as shown in Figure 26a. The other types of breaks do not show any correlation with low temperatures, and the normalized graph follows the day line (chapter 8.2 in the Appendix).

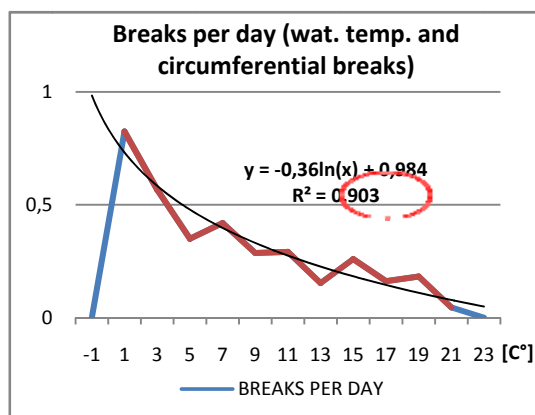


Figure 26a: Daily circumferential breaks with water temperature

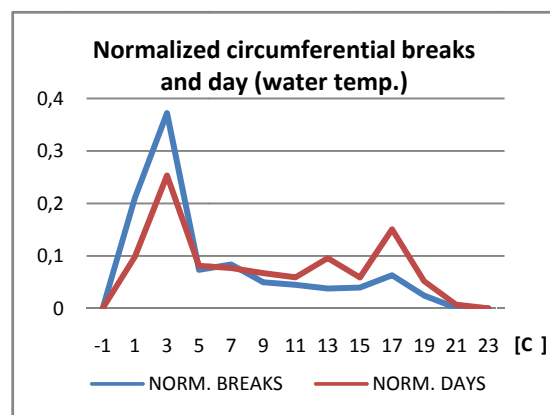


Figure 26b: Normalized circumferential breaks and normalized day with water temperature

Furthermore it is possible to observe that there is about one break per day when the weather is cold, compared to 0.6 when the temperature increases, Figure 27.

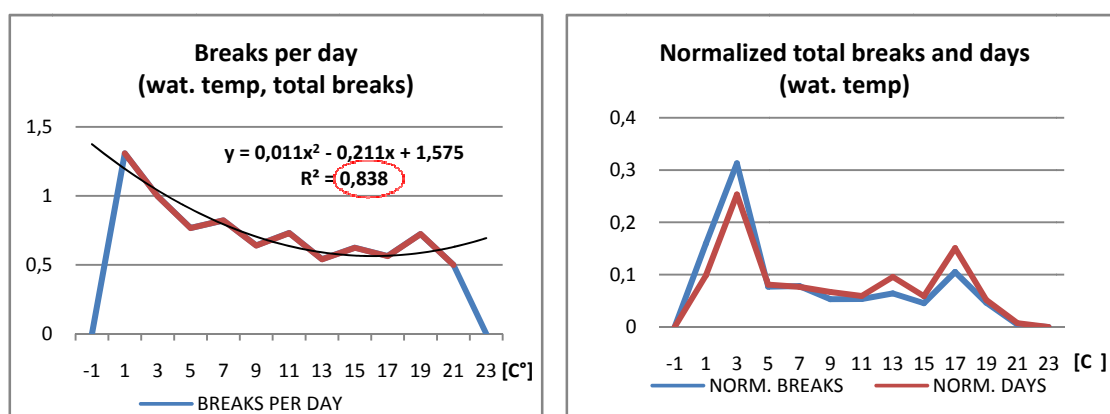


Figure 27a: Daily total breaks with air temperature

Figure 27b: Normalized total breaks and normalized day with air temperature

4.2.2.3 Correlation between temperature and breaks

The correlation between temperature and breaks was calculated using the software SPSS Statistics 17.0.

A correlation analysis was carried out for each of the variables. The software assesses the possible correlation between two variables at a time. It shows the degree to which the variables are related.

SPSS offers a choice between three kinds of correlations:

1. Pearson's correlation coefficient (r) is used to measure the strength of the linear association between two continuous variables;
2. Spearman rho is used to measure the strength of the monotonic association between two continuous variables. It is no more than a Pearson r computed on ranks and its significance can be tested just like r .
3. Kendall's tau coefficient (τ), which is based on the number of inversions (across X) in the rankings of Y, can also be used with rank data, and its significance can be tested.

Because the data is a non-continuous variable, the Kendall's tau coefficient was chosen.

The star shows the significance level:

One star (*) means that the correlation is significant at the 0.05 level;

Two stars (**) mean that the correlation is significant at the 0.01 level.

It is important to clarify that in statistics, significant means that something is probably true. The significance level is the probability that the null hypothesis is rejected when it is true and is an attribute of the distribution of a statistic test. It is usually denominated by the Greek letter α , and the most common levels of significance are 0.001 (0.1%), 0.01 (1%) and 0.05 (5%). They show how likely it is that a result is due

to chance; if the significant level is set to 0.05 for example, there is a 5% chance that the result is not true [19], [20].

Table 5: Results of correlations by SPSS Statistics 17.0

	AirTemp	WaterTemp
	Kendall's τ_b	Kendall's τ_b
CB01	-,096	-,109
TOTB01	-,126*	-,134*
CB02	-,167*	-,171*
TOTB02	-,177**	-,140**
CB03	-,097	-,222**
TOTB03	-,161**	-,244**
CB04	-,008	-,037
TOTB04	-,076	-,075
CB05	-,070	-,131
TOTB05	-,194**	-,185**
CB06	-,135	-,094
TOTB06	-,089	-,088
CB07	-,098	-,130
TOTB07	-,096	-,104
CB08	-,198*	-,195*
TOTB08	-,253**	-,241**
CB09	-,363*	-,533**
TOTB09	-,169	-,246**
CBBtot	,015	-,151**
TOTBtot	-,030*	-,141**

Table 5 shows the high correlation between low temperatures and breaks. Values in green are stronger than those in yellow. For some years (2004, 2006, 2007) there is no correlation. A possible explanation could be that in these years the pipes were stronger, due to the fact that the weakest pipes were replaced in the previous years because of breaks.

4.3 Pipe-soil interaction

The pipe-soil interaction analysis was conducted on grey and ductile iron pipes used in the Gothenburg network. Reference data used to calculate the stresses and strains on the pipes is shown in Table 6.

Table 6: Reference data for GI and DI pipes

Pipe geometry	Grey Iron (GI)	Ductile Iron (DI)
Diameter Nominal (DN)	100 mm	200 mm
Wall thickness (t)	9 mm	6,4 mm
Pipe length	5 m	6 m
Material properties		
Elastic modulus E_p	206000 MPa	165000 MPa
Ultimate tensile strength	207 MPa	290 MPa
Poisson's ratio ν	0,26	0,28
Thermal coefficient α_p	$10,5 \cdot 10^{-6} \frac{1}{^\circ C}$	$11 \cdot 10^{-6} \frac{1}{^\circ C}$
Operating conditions		
Water pressure	0,4 MPa	
Temperature differential ΔT	$\pm 15 \text{ } ^\circ C$	

Table 7 reports the range of elastic modulus of the soils E_s considered in the study, Poisson's ratio and k_s . The values for E_s and Poisson's ratio come from USACE [21] whereas the values for k_s are simply assumed based on the values shown in Table 8. The two soils highlighted are the two used in the calculations of the stresses on the ductile iron and grey iron pipe.

Table 7: Reference data for different kinds of soil

SOIL	E_s [MPa]		ν_s	k_s [MPa/m]
<i>Very soft clay</i>	0,5	5	0,5	20
<i>Soft clay</i>	5	20	0,45	
<i>Medium clay</i>	20	50	0,4	50
<i>Stiff clay- silty clay</i>	50	100	0,35	
<i>Sandy clay</i>	25	100	0,3	75
<i>Clay shale</i>	100	200		
<i>Loose sand</i>	10	25	0,3	120
<i>Dense sand</i>	25	100	0,2	
<i>Dense sand and gravel</i>	100	200	0,3	150
<i>Silty sand</i>	25	200		

The values for the pipe-soil reaction module were chosen based on the intervals indicated in Rajani's work. The 1996 study reports the same intervals as Table 8.

Table 8: Range of values for axial pipe-soil reaction module[14]

Axial pipe-soil stiffness [MPa/m]		
Soil type	Elastic response <i>[eq. (2)]</i>	CGL <i>[eqs. (3) and (4)]</i>
Clay	20-600	600-1200
Sand	120-180	

Figures 28 and 29 show the axial stress on the pipe for grey and ductile iron in dense sand and gravel, or medium clay. These graphs clearly indicate that clay causes less stress. It is important to point out that this result is based on the values chosen for the calculations. These values were selected in the absence of real data about the soil in Gothenburg, in order for this study to be carried out. It would definitely be useful to have more accurate data, to enable us to carry out a more exact study.

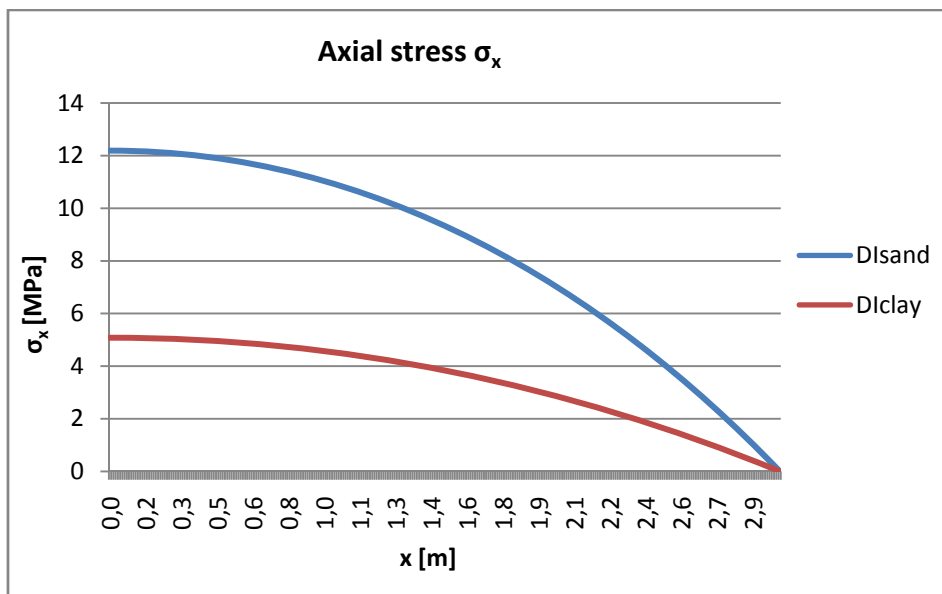


Figure 28: Results of axial stress for ductile iron pipe used in Gothenburg, in sand and clay

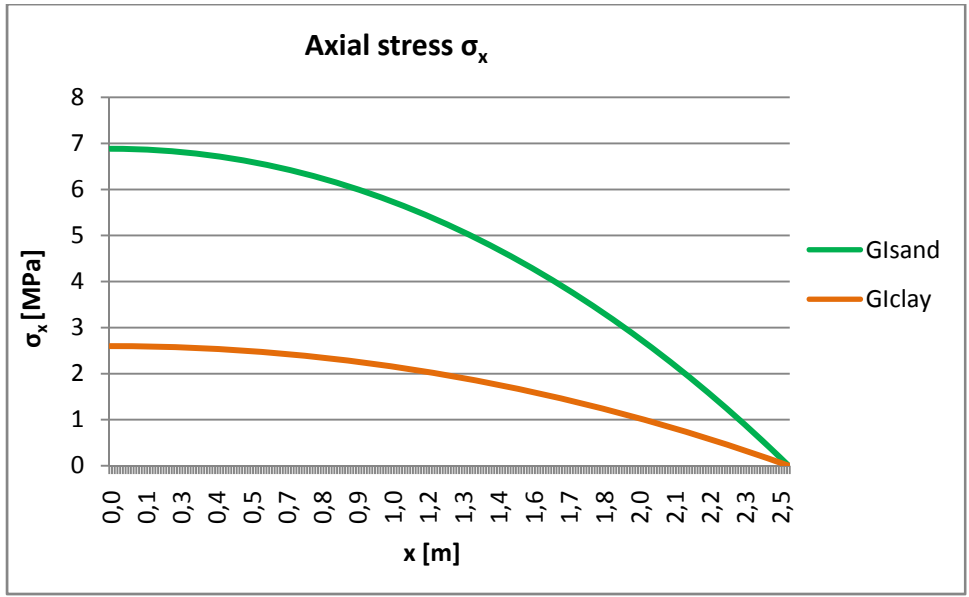


Figure 29: Results of axial stress for grey iron pipe used in Gothenburg, in sand and clay

Figure 30 illustrates the strain in ductile iron and sand. The strain depends on a combination of three factors; axial pipe resistance, water and earth radial pressure, and temperature changes. The biggest part of the strain is generated by the last factor. We decided to calculate the strain based on a temperature difference of 15°C degrees. This means that the pipe was buried at a temperature of 20°C, and is analysed at a temperature of 5°C.

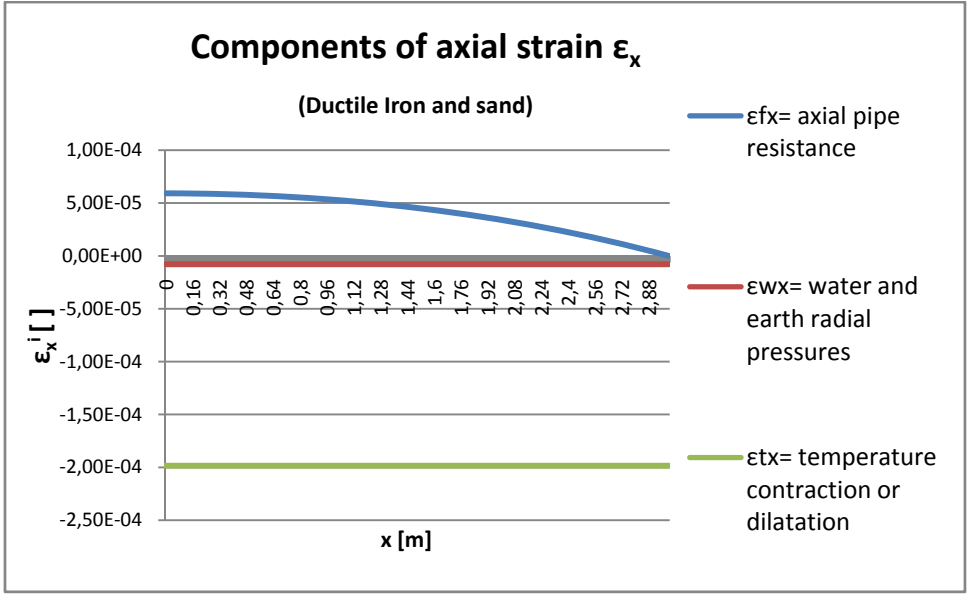


Figure 20: Components of axial strain in ductile iron and sand

4.3.1 Sensitivity analysis

The response of jointed water mains pipes obtained above can be used to conduct a sensitivity analysis in order to identify the influence of the key variables on the answer.

Strains and stresses depend on many different variables, why it is necessary to vary one variable at a time and study how this affects the result, to understand how each of the key parameters and variables impact on the stress and strain. The problem chosen and taken as example is reported in Table 7 for pipe materials and sizes, and in Table 8 for soil properties.

To begin with, the axial pipe-soil response as a function of the k parameter introduced in Equation (22) was evaluated. The key variables affecting the k parameter are D/t and E_s/E_p , whereas the Poisson's ratios for pipe and soil are less important influences. The maximum axial stress, that is at mid-span, obtained from Equations (23) (24) and (25), is shown.

The graphs in Figures 31 and 32 below show how k varies with the ratio D/t of the pipes and different soils, for grey iron and ductile iron. It should be noticed that the interaction factor k does not vary significantly with the D/t ratio and that there is not much difference between how ductile iron and grey iron interact with the soil.

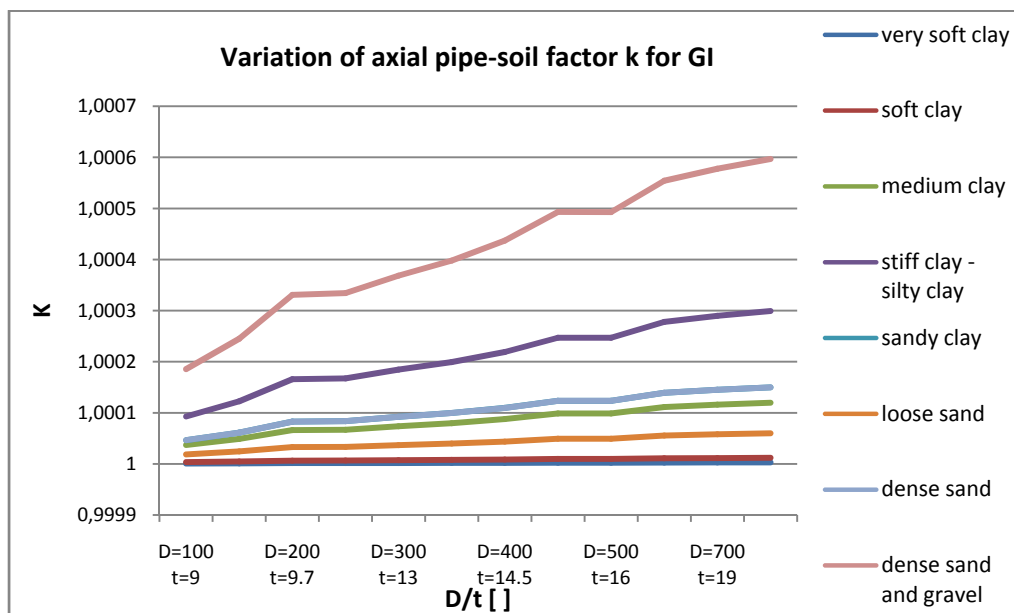


Figure 31: Variation of axial pipe-soil factor for standard ratio of diameter and thickness of grey iron pipes

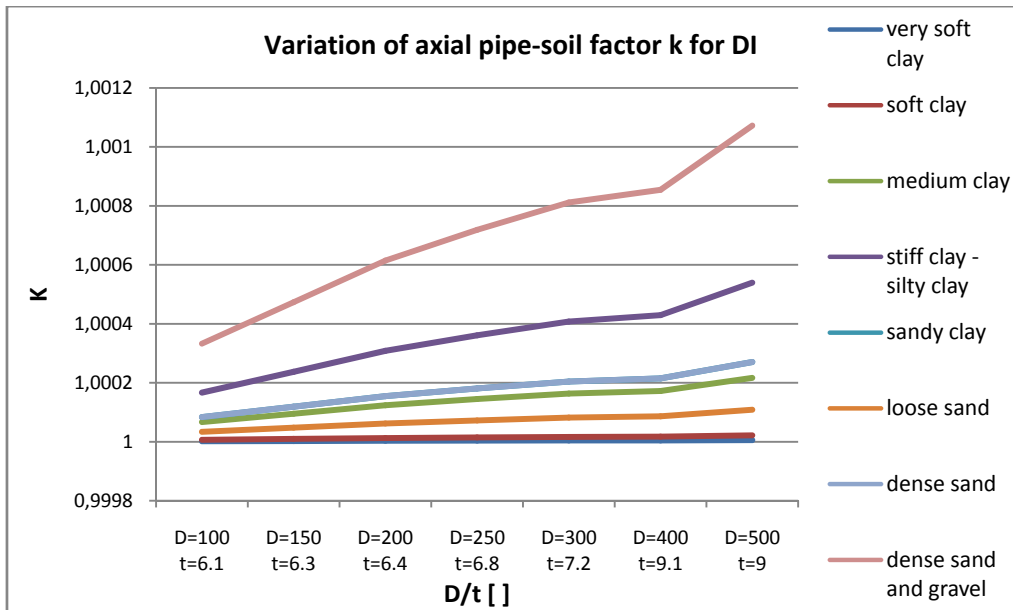


Figure 32: Variation of axial pipe-soil factor for standard ratio of diameter and thickness of ductile iron pipes

Figures 33 and 34 show, for ductile iron and grey iron pipes respectively, how the hoop stress varies with the D/t and pipe-soil elastic module ratio (E_p/E_s). The response is such that the pipe does not feel the radial restraint of the surrounding backfill, except in cases where the pipe-soil elastic module ratio (E_p/E_s) is very low.

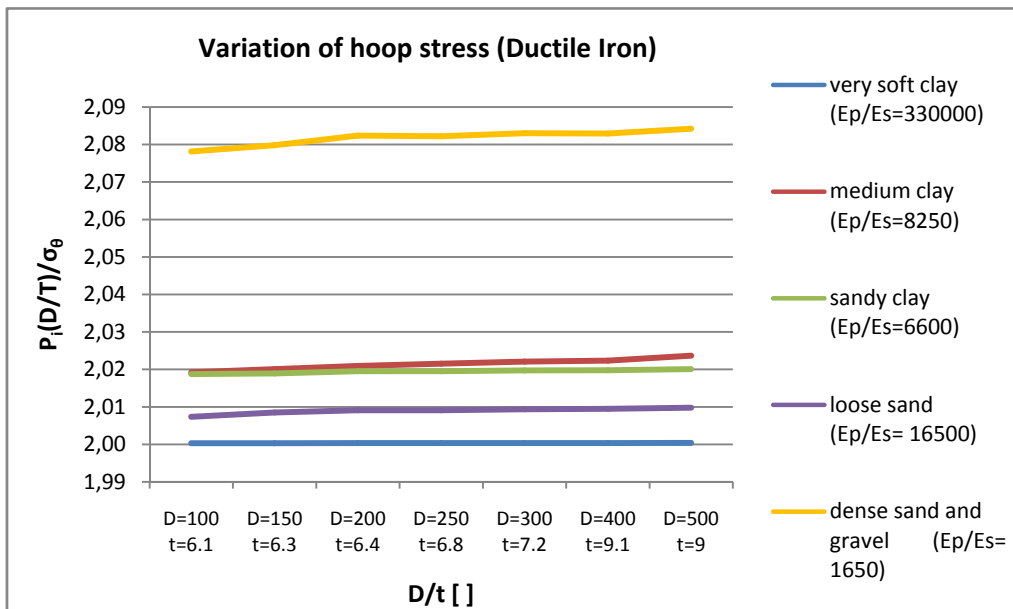


Figure 33: Variation of hoop stress for standard ratio of diameter and thickness of ductile iron pipes and different ratio of Young module of pipe and soil

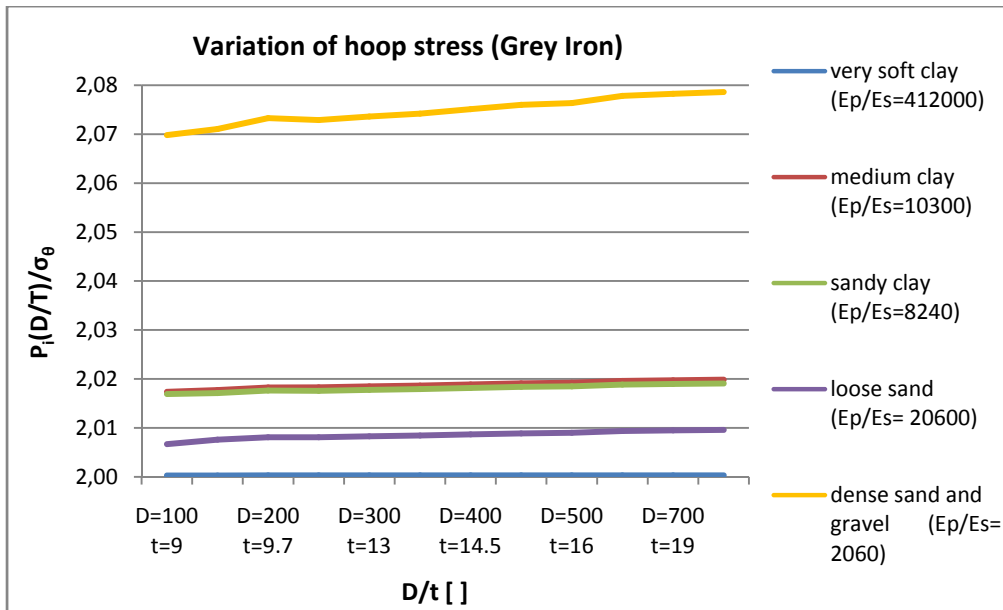


Figure 34: Variation of hoop stress for standard ratio of diameter and thickness of grey iron pipes and different ratio of Young's module of pipe and soil

Based on data on pipe sizes used in Gothenburg, the influence of D/t ratio on maximum axial stress at mid-span was studied. The findings are shown in Figures 35 and 36. This confirms that the smallest pipes are subjected to greater stress, and this is why they break the most.

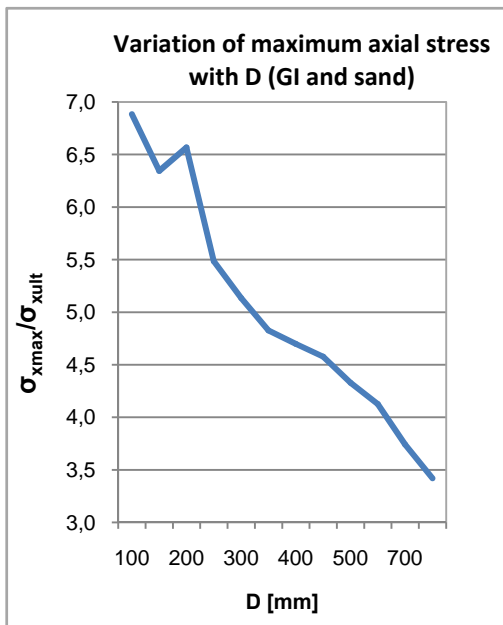


Figure 35: Variation of maximum axial stress for different sizes of grey iron pipes

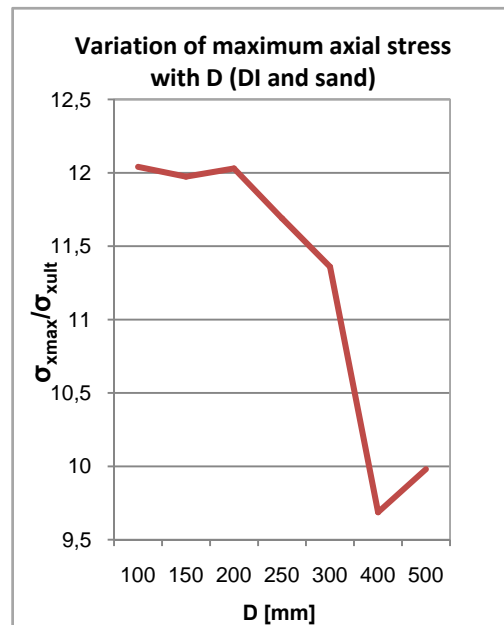


Figure 36: Variation of maximum axial stress for different sizes of ductile iron pipes

Figures 37 and 38 show the variation of the axial stress along the pipe, from the mid-span to the end. The calculations were based on the reference problem (Table 6), varying the kind of soils and consequently the ratio E_p/E_s .

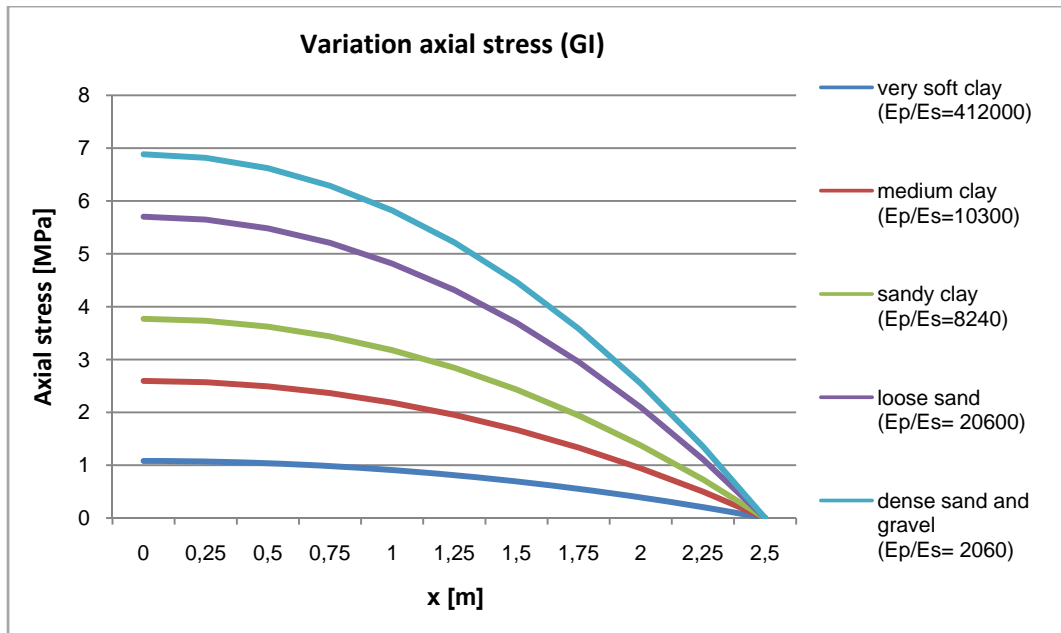


Figure 37: Variation of axial stress along the pipe for ratio of Young's module of grey iron and different kinds of soil

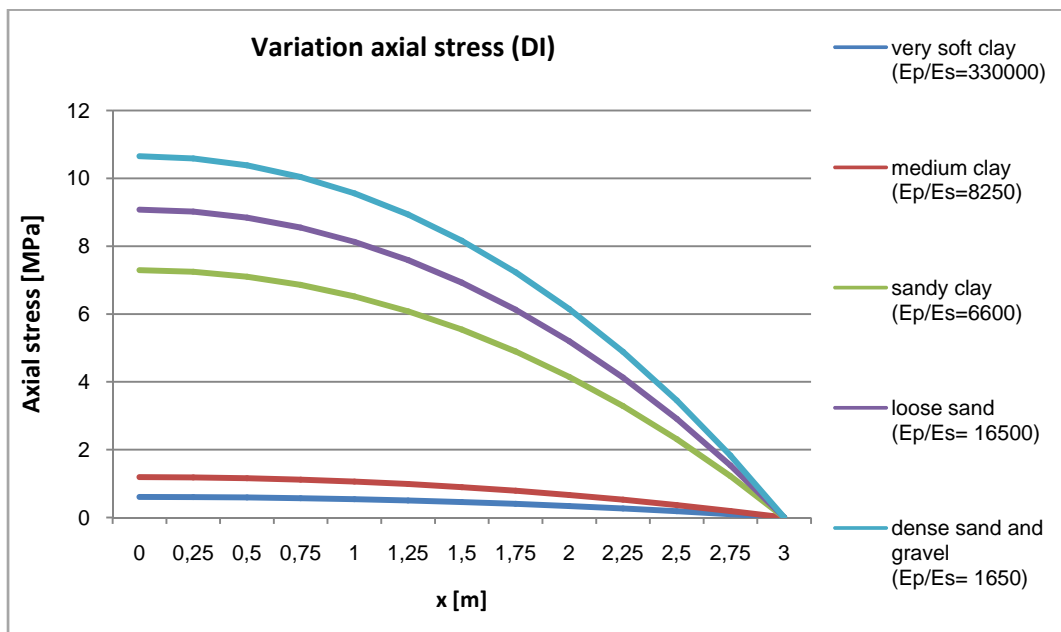


Figure38: Variation of axial stress along the pipe for ratio of Young's module of ductile iron and different kinds of soil

It looks like the clay soils bring less stress, but this is due to the chosen values of k_s . The values were set lower than the sand values, in the range shown in Table 8, and this is the reason why there was less stress. To obtain more reliable results, it would be necessary to have real data on these values, which strongly influence the results. In fact, as showed in Figure 39, the influence of the axial pipe-soil restraint k_s , still calculated at mid-span, is high. The variation in axial stress was calculated for ductile iron water mains with the characteristics outlined in Table 6, and in a medium clay soil.

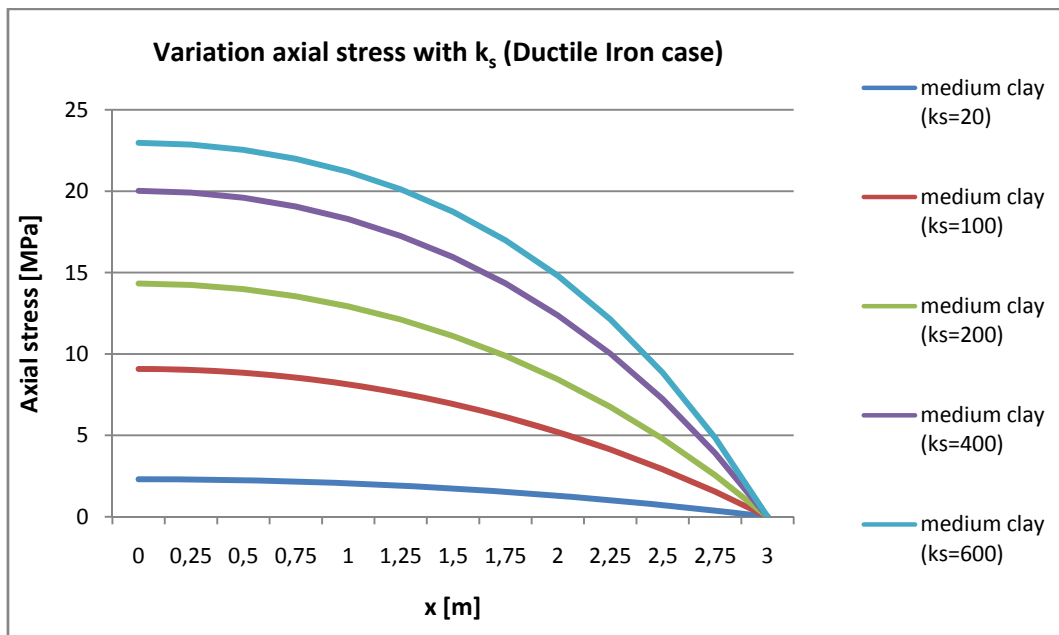


Figure 39: Variation of axial stress for different values of modulus k_s

Figure 40 shows how the maximum axial stress (compared with the ultimate tensile strength) varies with extreme temperatures. This was calculated for the two soils considered in the study. The ultimate strength is the maximum stress a material can withstand when subjected to tension, compression or shearing. It is the maximum stress on the stress-strain curve. Thus the ultimate tensile strength is the maximum stress that a material subjected to tension can resist.

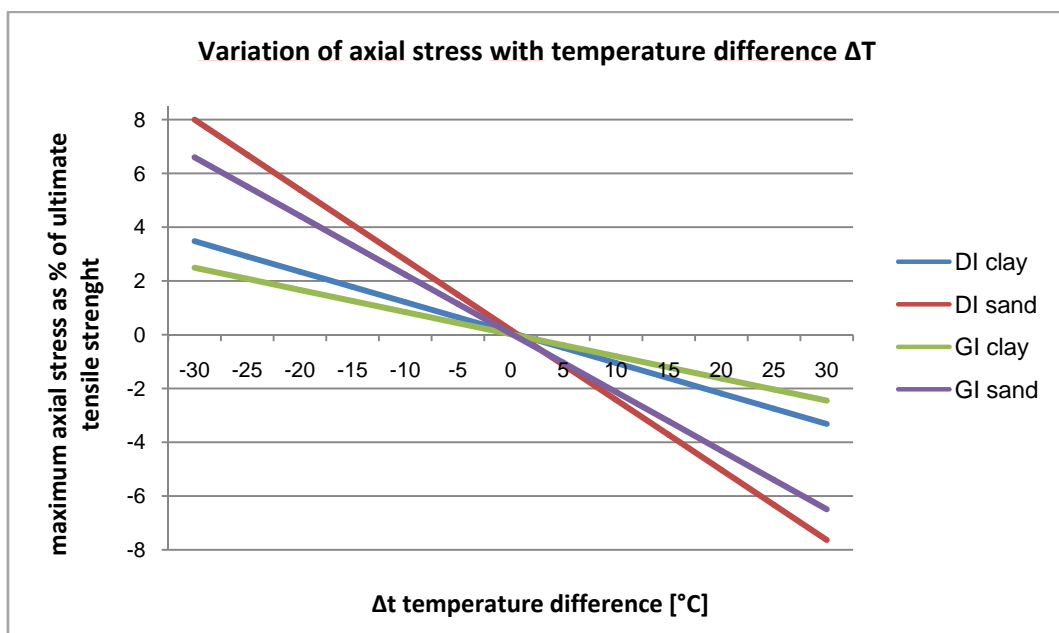


Figure 40: Influence of temperature extremes on maximum axial stress for different pipe materials and soils

Figures 41 and 42 show how the axial stress varies with the changes in temperature over time. The ground temperature over a 12-month period can be adequately represented [14] as a function of time, t by the equation:

$$T(t) = T_m + A^T \cos\left(\frac{2\pi t}{365}\right)$$

where A^T (5 °C) is the amplitude of the temperature change and T_m (5,5 °C) is the mean temperature. Because a high number of pipe breaks is observed during the winter, or the cold season, it is interesting to study variations in the temperature amplitude A^T , to simulate the extremes of seasonal temperatures. Figures 41 and 42 show how the axial stress changes as the temperature varies, for a grey and ductile iron pipe respectively. This analysis demonstrates that an increase in circular pipe breaks maybe due to cold ground temperatures. Moreover, the stress may have detrimental effects on corroded water mains.

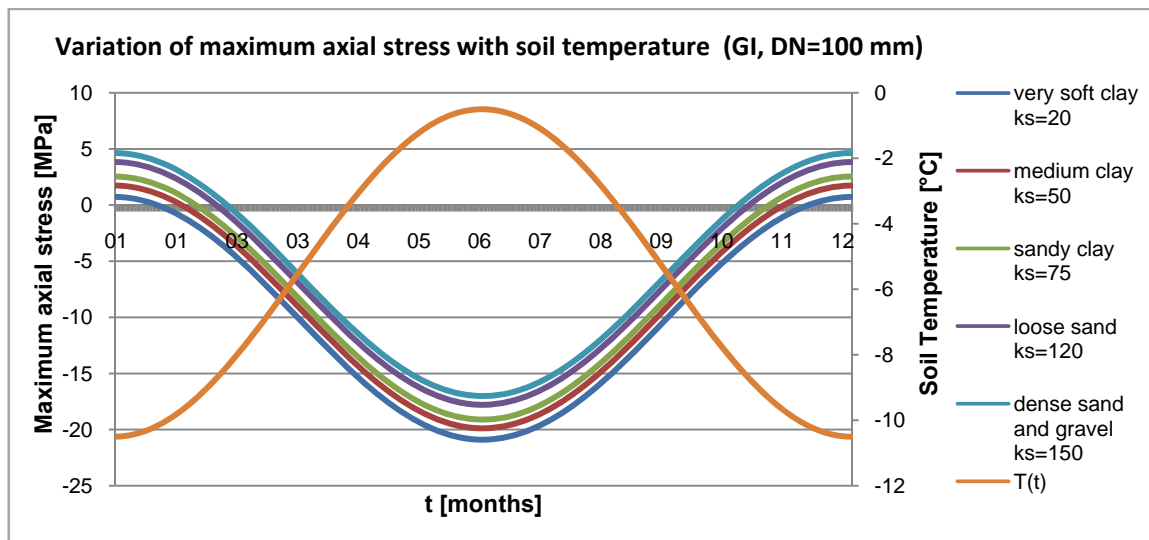


Figure 41: Variation of maximum axial stress with soil temperature, for different kinds of soil and a grey iron pipe with a diameter of 100 mm

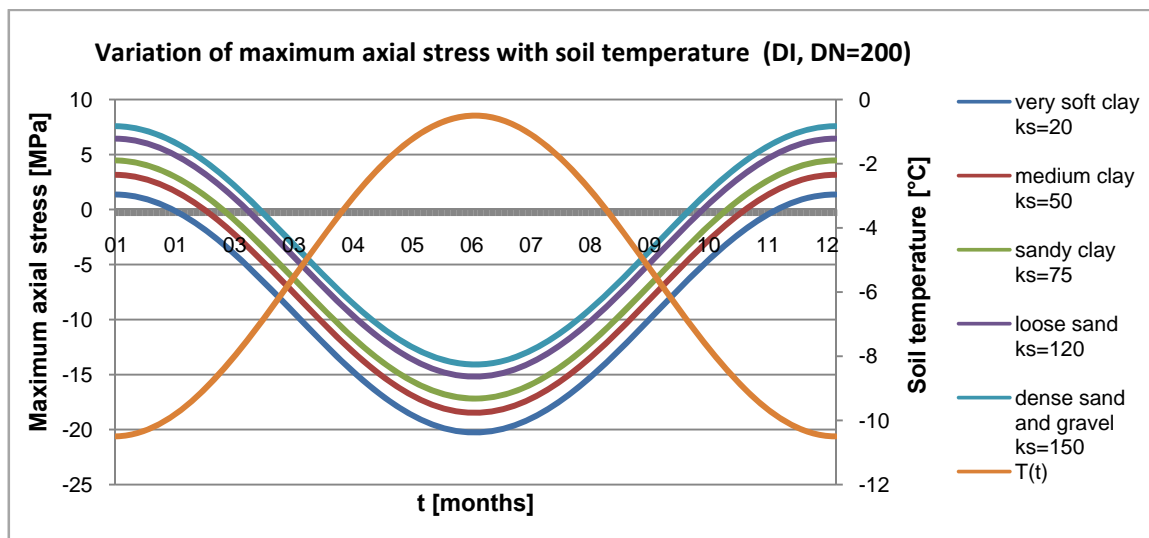


Figure 42: Variation of maximum axial stress with soil temperature and for different kinds of soil and a ductile iron pipe with a diameter of 200 mm

5 Further data

Additional data, especially about the soil, is required. Several conclusions were reached in this thesis, but with access to more data, it would be possible to produce a better and more useful report.

The water temperature data is not from the treatment plants where the water is put into the network, but instead comes from Lake Delsjön. Water temperatures were available from Alelyckan and Lackarebäck waterworks, however not broken down by date. The temperatures recorded by the treatment plants are more variable, and it is likely that the correlation would have been higher than shown here had this data been used. This is why it would be desirable to have accurate temperature data from the plants or, even better, data on the temperature of the water inside the pipes. The water temperature is more important than the air temperature, as it is in direct contact with the pipes, and, as shown in this thesis, the former is more closely correlated with the number of breaks.

The most common type of break is the circumferential break. It is known that circumferential breaks are caused by longitudinal stress. It would be useful to have data on soil temperatures in Gothenburg, because if the actual temperature of the water and soil were known, it would be possible to conduct a study about the linear trend of the temperature variation. If the temperature inside the pipe was lower than the temperature on the outside, the pipe would be subjected to bending stress. For instance, with a water temperature of 10°C and a soil temperature of 5°C, pipes will be subjected to a positive bending stress; during the winter the pipe maybe subjected to an opposite bending stress as the temperature of the water would be lower than that of the soil. This change of direction cannot be withstood by an iron pipe. Moreover, it is possible that the strain of the pipe is plastic; this means that the pipe is subjected to a deformation that is increasing year by year. With more information about water and soil temperatures, it would also be possible to carry out a study into the bending action on the pipes.

It is definitely necessary to have more knowledge about Gothenburg's ground. All the calculations carried out in this study were based on assumptions about the soil. This is the reason why the calculations were done either for sand or for clay. On the one hand, we know that Gothenburg is mainly built on clay, but on the other hand, sand has lately been used as backfill. Furthermore, by studying the stresses caused by pipe-soil interaction, it has been proven, that clays induce less stress on the pipe; this finding is valid only for clays with low k_s values. It is appropriate at this point to remember and underline the ability of soils to retain salts. These may have an unfavourable effect through increasing the corrosion rate of cast iron pipes by the creation of galvanic cells. One of the salts with the most devastating effects is sodium chloride, NaCl. It is possible that salts are present in Gothenburg's soils because of the nearness of the sea. Moreover, NaCl is present in the de-icing reagents applied directly to roads in winter and may penetrate to the pipes, even though gravel is used as much as possible.

To study the salt concentration in the soil, resistivity could be used, that is the ability of a conductive material to withstand electrical current, or, more precisely, the electrical resistance between the opposite faces of a unit cube of material. With a higher salt concentration the ability of the soil to conduct increases, and therefore the resistivity is lower. For this reason, a soil with a low resistivity has a higher potential

for corrosion. A classification of resistivity standard values and relative corrosiveness is given in Table 9 [15].

Table 9: Soil corrosiveness as a function of resistivity [10]

Soil resistivity [$\Omega\cdot\text{cm}$]	Types of soil	Expected corrosiveness
>20000	Sand	<i>Virtually non aggressive</i>
10000 – 20000	Sand	<i>Weakly aggressive</i>
5000 – 10000	Loam	<i>Moderately aggressive</i>
3000 – 5000	Loam, peat	<i>Aggressive</i>
1000 – 3000	Clay, peat	<i>Strongly aggressive</i>
500 – 1000	Brackish, clay	<i>Very strongly aggressive</i>
<500	Clay	<i>Extremely aggressive</i>

The knowledge about soil is very important, as this is the material nearest the pipe, after the one used as backfill. Also, as shown in Table 9, it is correlated to the pipe's corrosion. The consequence of this could be a loss in pipe resistance. Seica et al. [15] carried out several tests on new and corroded pipes, to better understand the behaviour of the pipes and the influence of corrosion on the resistance and on the loss of strength of iron materials. This study shows a loss of theoretic initial strength from a minimum value of 0.3 % up to 52 %. This is especially true for those pipes that have lost metallic material because of corrosion. It was also shown that a possible cause of lower strength is manufacturing defects, such as the presence of air inclusions, which occur fairly frequently in older pipes, and is due to the manufacturing technology used for specific pipes at certain times.

5.1 Considerations on melting snow

A last consideration is illustrated in Figure 43.

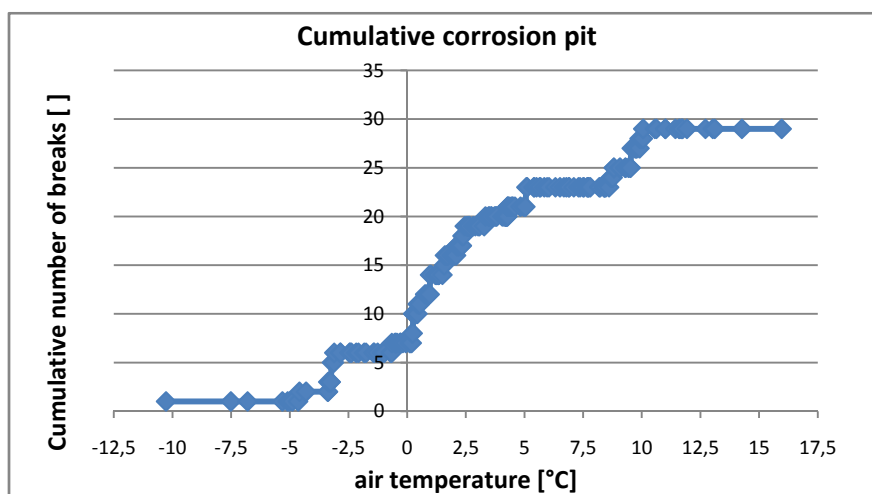


Figure 43: Cumulative distribution of corrosion pit breaks with air temperature

The figure shows the cumulative distribution of corrosion pit breaks that occurred between October 2008 and April 2009, with increasing air temperature.

It is possible to notice that the greatest number of breaks occur at temperatures between 0°C and 3°C. This interval corresponds to the snow melting, and it would be interesting to analyse whether a correlation exists between the corrosion breaks and the melting of the snow, considering the large amounts of snow that fall during the long winter and the fact that Gothenburg is an industrial city. In fact, it may be the case that a large quantity of pollution agents permeates the ground when the snow melts.

6 Conclusions

From the analysis of the types of break and materials that was carried out, it can be deduced that the most frequently broken pipes in the Gothenburg network are made of grey iron. The most common type of break is the circumferential break. It is known that circumferential breaks are caused by longitudinal stress. It would be really useful to have data on soil temperature in Gothenburg, as knowledge of the actual soil and water temperatures would make it possible to carry out a study about the linear trend of the temperature variations.

The correlation study shows that the number of breaks increases as the temperature decreases. For most of the years considered, there is a correlation with the temperatures, especially with the water temperature. The years 2004, 2006 and 2007 do not show any correlation either with air nor water temperature. It is possible that these results derive from the replacement of weak pipes in the previous years, and due to the greater strength of the new pipes, the network had fewer breaks in those years. Data on where pipes have been replaced would make it possible to prove whether the absence of correlation is due to the substitution of weak pipes in the previous years.

The sensitivity analysis showed that the pipes with the smallest diameter were more likely to break. This confirms the data analysis of Gothenburg's water mains, which found that the weakest pipes have diameters of 100 mm and 200 mm for grey iron and ductile iron respectively. The reason for this is probably the smaller contact area with the soil, which causes greater stresses on the pipes. This study also looked at the influence of soil properties on the axial pipe stress, which is the cause of circumferential breaks. These occur more often during the cold season, because the axial stress is strongly related to the temperature variation and the axial pipe-soil reaction modulus k_s . This is not true, however, for the hoop stress that causes longitudinal breaks, because it is not influenced by changes in the key variables. The discussion of axial or hoop stresses is always made in reference to intact pipe material, however, metallic pipes, such as grey and ductile iron, develop pits as a result of corrosion, losing theoretical ultimate strength.

To achieve a good water supply and a substantial saving in resources it is necessary to continue to study this topic, and to deepen our knowledge about the interaction between pipe and soil and the behaviour of materials.

7 References

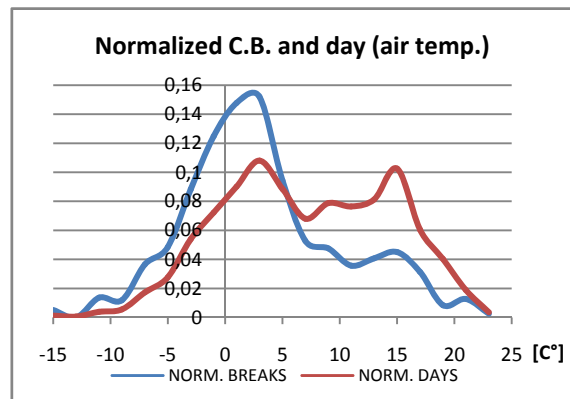
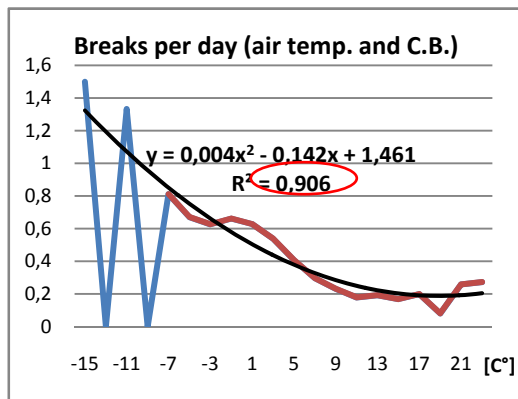
- [1] L.Andersson, Å.Bengtsson Sjörs, C.Jonelind (2006).Vattenledningar och vattenläckor: Variationen på dricksvattnets temperatur och dess betydelse för antalet vattenläckor (Waterpipes and failure rates: Drinking water temperature and its correlation to pipe failures) VA-Forskrapport, **No 2006-06**. *In Swedish*
- [2] M.-C.Besner, J.Lavoie, C.Morissette, P.Payment (2008). Effect of water main repairs on water quality. *American Water Works Association. Journal*; **100**, **No. 7**, 95-109.
- [3] C.M. Clark (1971). Expansive- soil effect on buried pipe. *Journal of the American Water Works Association*, **63**, 424-427.
- [4] Committee on Gas and Liquid Fuel Lifelines (1984). Guidelines for seismic design of oil and gas pipeline systems. *American Society of Civil Engineers*, New York.
- [5] A.Habibian, Effect of temperature changes on water-main breaks (1994). *Journal of Transportation Engineering*, **120**, **No. 2**, March-April.
- [6] D.A. Jesson, B.H. Le Page, M.J. Muhlheron, P.A. Smith, A. Wallen, R. Cocks, J. Farrow, J.T. Whiter (2010). Strains and stresses in cast iron pipes. *Journal of Water Supply*, **59**, **No. 4**, 221-229.
- [7] G.J.Kirmeyer, M. Friedman, K. Martel, D.Horwie, M.LeChevallier, M.Abbaszadegan, M. Karim, J. Funk, J.Harbour (2001). Pathogen intrusion into the distribution system. *American Water Work Association RF*, Denver.
- [8] V.Muñoz Mendel (2005). Raw Water Storage. Case study: Gothenburg's Water Supply.
- [9] R.E.Morris (1967). Principal causes and remedies of water main breaks. *Journal of American Water Work Association*, **54**, 782-798.
- [10]NRC (2006). Drinking Water Distribution System. *National Research Council of the National Academies, National Academies Press*.
- [11]K. Nygård, E. Wahl, T. Krogh, O. A.Tveit, E.Bøhlenh, A.Tverdal, P.Aavitsland (2007). Breaks and maintenance work in the water distribution system and gastrointestinal illness: a cohort study. *International Journal of Epidemiology*, **36**, 873-880.
- [12]B.Rajani, Y.Kleiner (2001). Comprehensive review of structural deterioration of water mains: physically based models. *Urban Water*, 3, 151-164.

- [13] B.Rajani, S.Tesfamariam (2004). Uncoupled axial, flexural, and circumferential pipe–soil interaction analyses of partially supported jointed water mains. *Canadian Geotechnical Journal*, **41**, 997-1010.
- [14] B.Rajani, C.Zhan, S.Kuraoka (1996). Pipe-soil interaction analysis of jointed water mains. *Canadian Geotechnical Journal*, **33**, 393-404.
- [15] M.V.Seica, J.A.Packer, M.W.F.Grabinsky, B.J.Adams (2002). Evaluation of the properties of Toronto iron water mains and surrounding soil. *Canadian Journal of Civil Engineering*, **9**, 222-237.
- [16] R. F. Scott (1981). *Foundation Analysis*. Prentice Hall, New Jersey.
- [17] S.Tesfamariam, B.Rajani, R.Sadiq (2006). Possibilistic approach for consideration of uncertainties to estimates structural capacity of ageing cast iron water mains. *Canadian Journal of Civil Engineering*, **33**, 1050-1064.
- [18] T.Westrell, O.Bergstedt, T.A.Stenström, N.J.Ashbolt (2003). A theoretical approach to assess microbial risks due to failures in drinking water systems. *International Journal of Environmental Health Research*, **13**, 181-197.
- [19] <http://en.wikipedia.org/2010/05/24>
- [20] <http://economics.about.com/od/2010/05/24>
- [21] www.geotechnicalinfo.com/2010/06/01

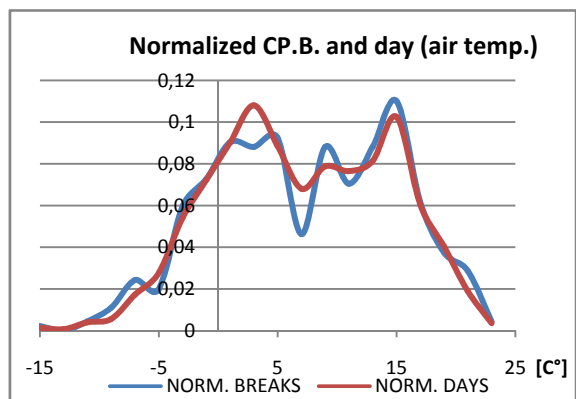
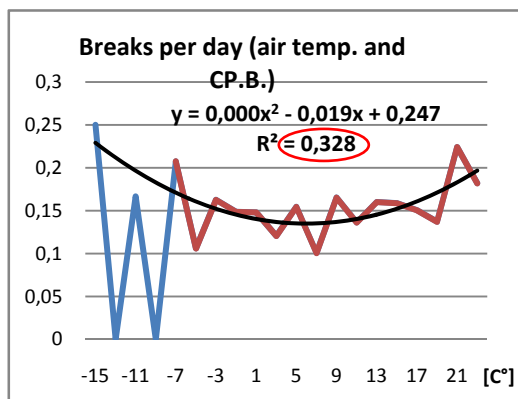
8 Appendix

Graphs of break and air temperature

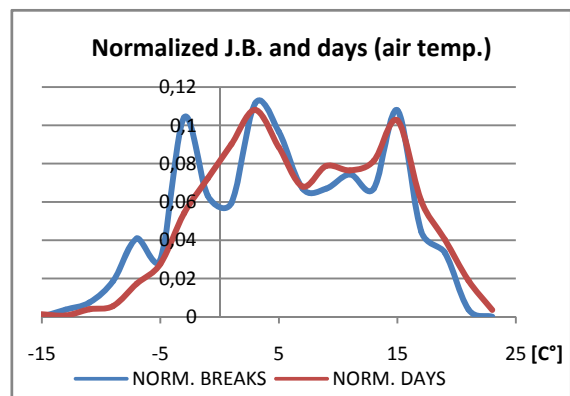
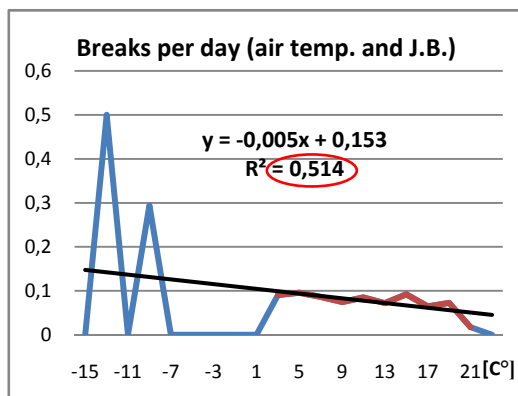
Circumferential breaks



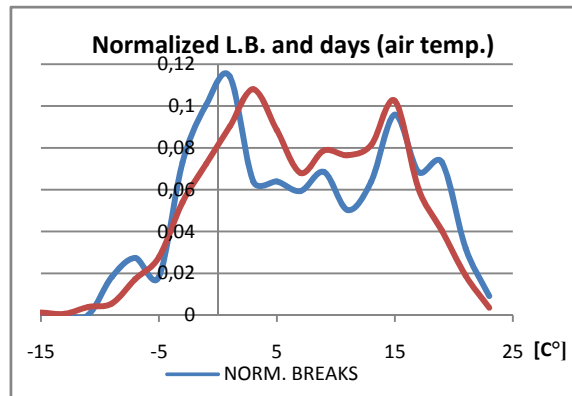
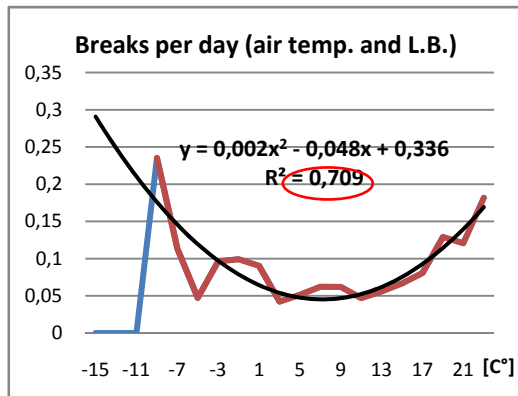
Corrosion pit breaks



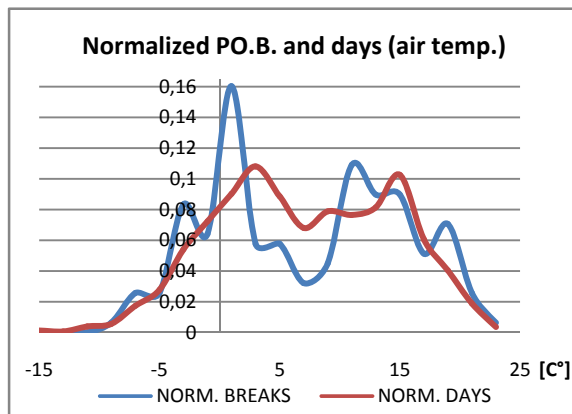
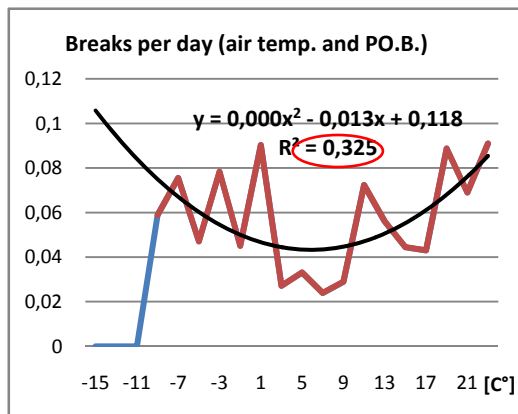
Joint breaks



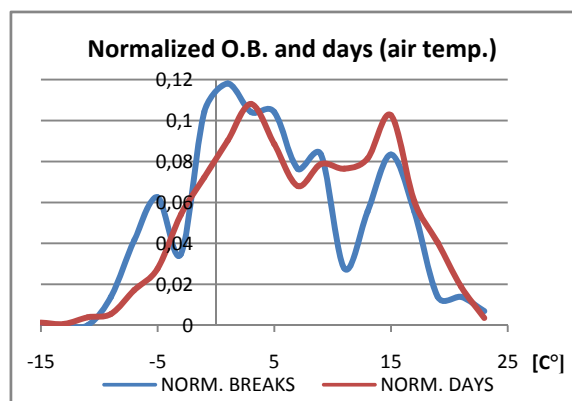
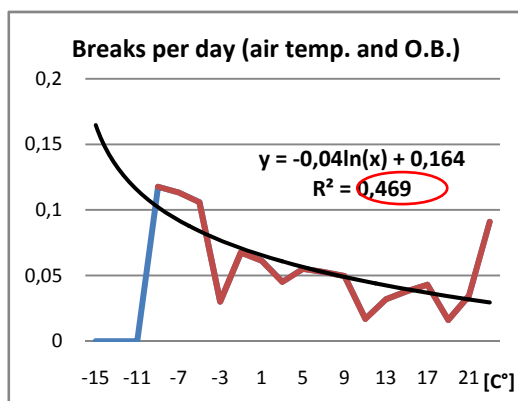
Longitudinal breaks



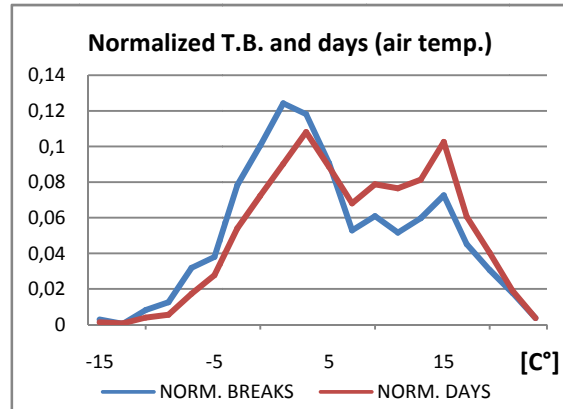
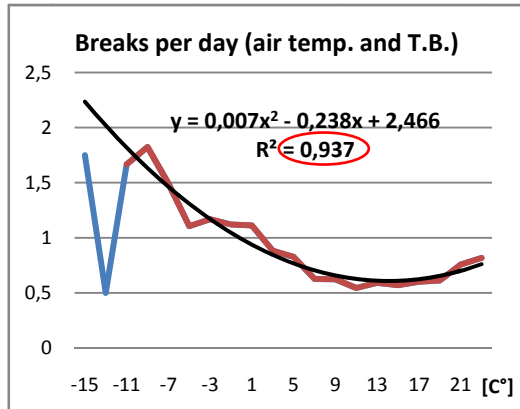
Piece out breaks



Other breaks

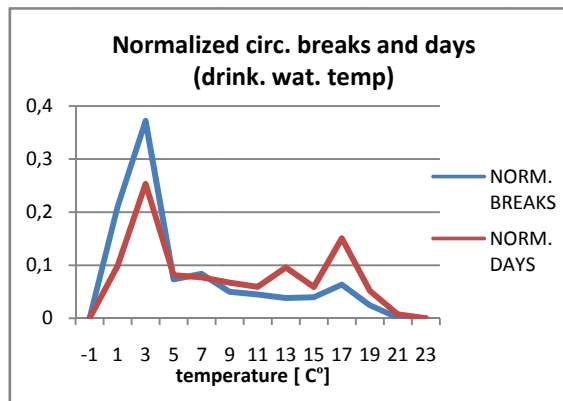
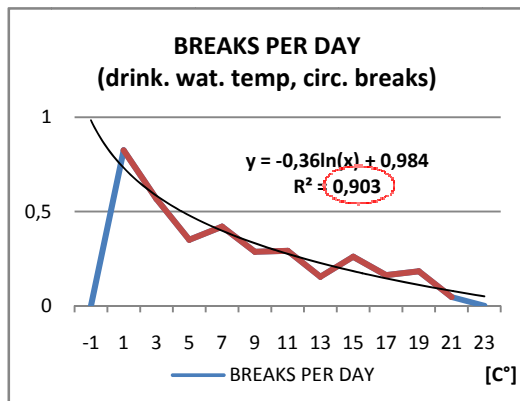


Total breaks

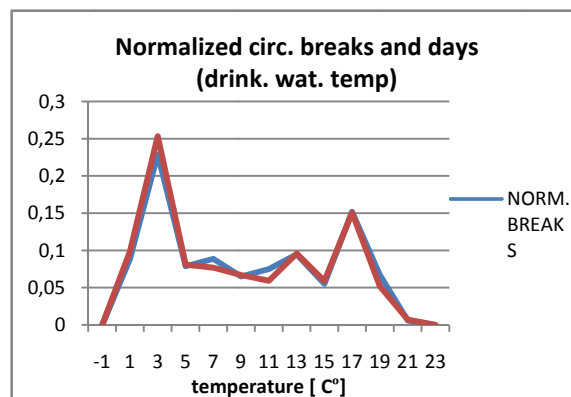
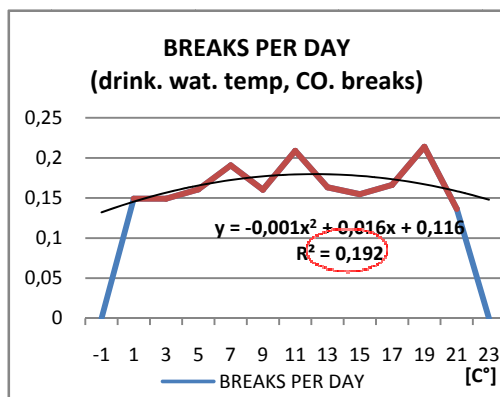


1.2. Graphs of breaks and water temperature

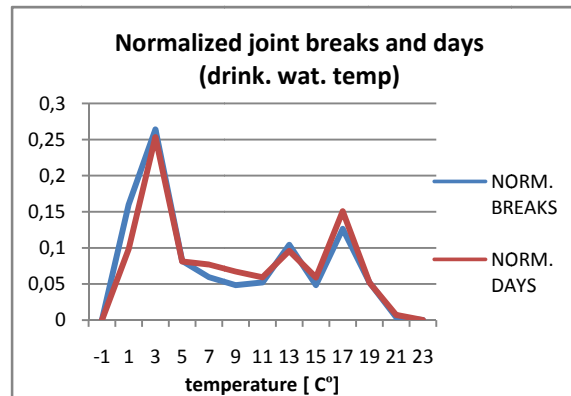
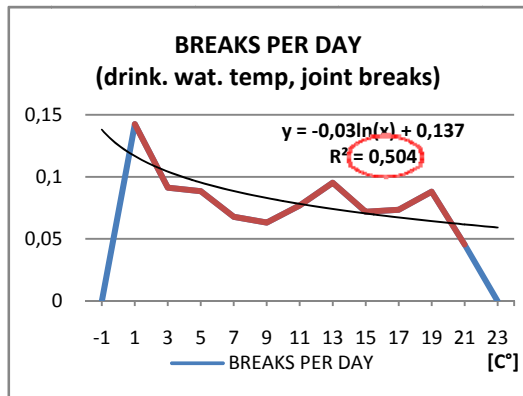
1.2.1. Circumferential breaks



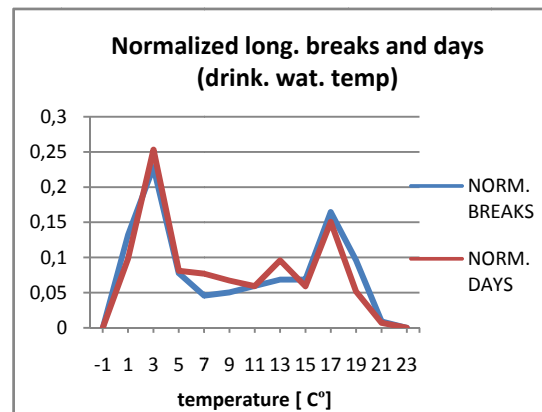
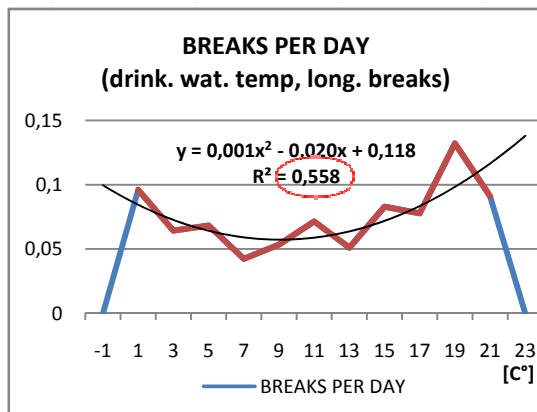
Corrosion pit breaks



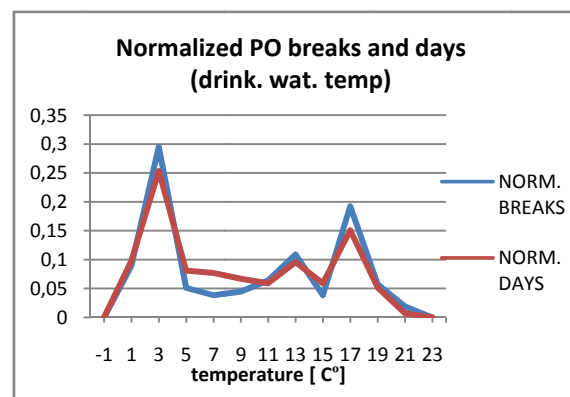
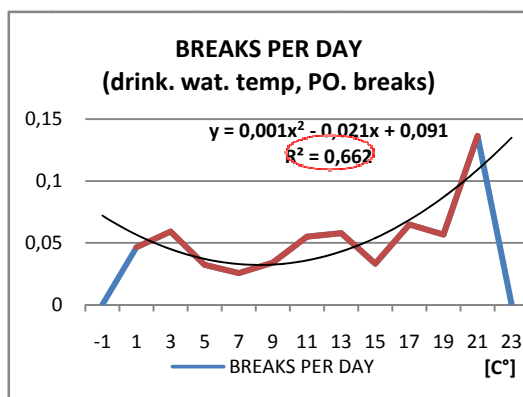
Joint breaks



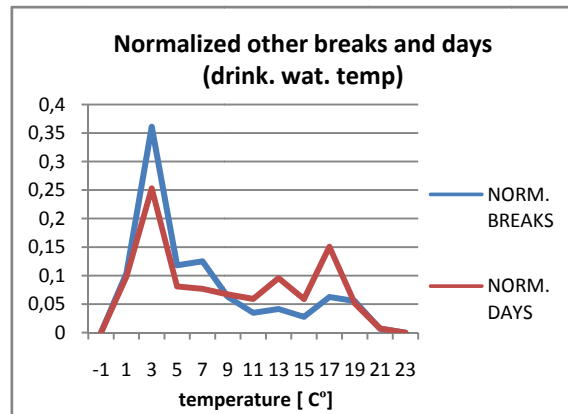
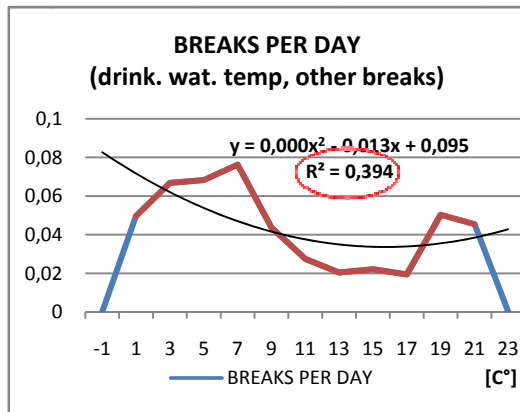
Longitudinal breaks



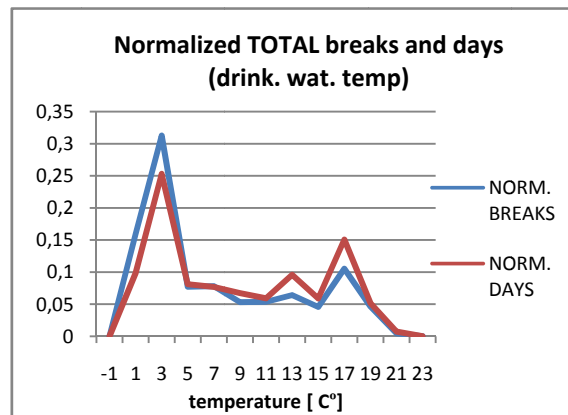
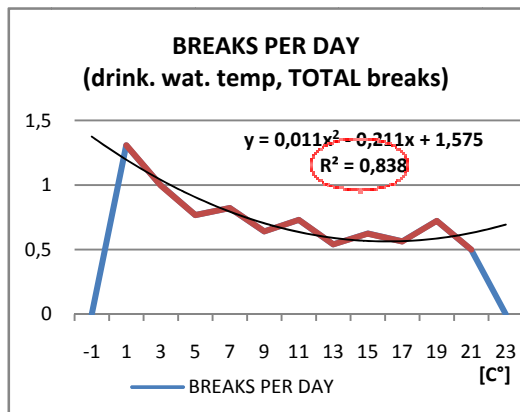
Piece out of pipe breaks



Other breaks



Total breaks



Correlation by SPSS Statistics 17.0

Results of the year 2001

Correlations					
			TOTB01	AirTemp01	WaterTemp01
Kendall's tau_b	CB01	Correlation Coefficient	,654**	-,096	-,109
		Sig. (2-tailed)	,000	,192	,139
		N	117	117	116
	CPB01	Correlation Coefficient	,366**	-,079	-,074
		Sig. (2-tailed)	,002	,456	,484
		N	62	62	62
	JB01	Correlation Coefficient	.	.	.
		Sig. (2-tailed)	.	.	.
		N	21	21	21
	LB01	Correlation Coefficient	,292	,053	,196
		Sig. (2-tailed)	,100	,738	,220
		N	28	28	28
	POB01	Correlation Coefficient	,361	,000	-,171
		Sig. (2-tailed)	,199	1,000	,527
		N	11	11	11
	OB01	Correlation Coefficient	.	.	.
		Sig. (2-tailed)	.	.	.
		N	1	1	1
	TOTB01	Correlation Coefficient	1,000	-,126*	-,134*
		Sig. (2-tailed)	.	,029	,021
		N	181	181	180
AirTemp01	Correlation Coefficient	-,126*	1,000	,691**	
	Sig. (2-tailed)	,029	.	,000	
	N	181	365	364	
WaterTemp01	Correlation Coefficient	-,134*	,691**	1,000	
	Sig. (2-tailed)	,021	,000	.	
	N	180	364	364	
**. Correlation is significant at the 0.01 level (2-tailed).					
*. Correlation is significant at the 0.05 level (2-tailed).					

Results for the year 2002

Correlations					
			TOTB02	AirTemp02	WaterTemp02
Kendall's tau_b	CB02	Correlation Coefficient	,602**	-,167*	-,171*
		Sig. (2-tailed)	,000	,021	,018
		N	118	118	118
	CPB02	Correlation Coefficient	,383**	,051	,069
		Sig. (2-tailed)	,000	,589	,460
		N	76	76	76
	JB02	Correlation Coefficient	,316*	-,175	-,021
		Sig. (2-tailed)	,038	,214	,879
		N	35	35	35
	LB02	Correlation Coefficient	,359*	-,024	,071
		Sig. (2-tailed)	,024	,871	,625
		N	33	33	33
	POB02	Correlation Coefficient	,313	,000	,129
		Sig. (2-tailed)	,169	1,000	,540
		N	17	17	17
	OB02	Correlation Coefficient	,248	,346	,577
		Sig. (2-tailed)	,546	,380	,143
		N	6	6	6
	TOTB02	Correlation Coefficient	1,000	-,177**	-,140**
		Sig. (2-tailed)	.	,001	,009
		N	202	202	202
AirTemp02	Correlation Coefficient	-,177**	1,000	,698**	
	Sig. (2-tailed)	,001	.	,000	
	N	202	365	365	
WaterTemp02	Correlation Coefficient	-,140**	,698**	1,000	
	Sig. (2-tailed)	,009	,000	.	
	N	202	365	365	
*. Correlation is significant at the 0.05 level (2-tailed).					
**. Correlation is significant at the 0.01 level (2-tailed).					

Results for the year 2003

Correlations					
			TOTB03	AirTemp03	WaterTemp03
Kendall's tau_b	CB03	Correlation Coefficient	,664**	-,097	-,222**
		Sig. (2-tailed)	,000	,174	,002
		N	123	123	123
	CPB03	Correlation Coefficient	,234	,017	,000
		Sig. (2-tailed)	,086	,890	1,000
		N	47	47	47
	JB03	Correlation Coefficient	,336*	-,033	,026
		Sig. (2-tailed)	,027	,808	,850
		N	38	38	38
	LB03	Correlation Coefficient	.	.	.
		Sig. (2-tailed)	.	.	.
		N	17	17	17
	POB03	Correlation Coefficient	.	.	.
		Sig. (2-tailed)	.	.	.
		N	12	12	12
	OB03	Correlation Coefficient	.	.	.
		Sig. (2-tailed)	.	.	.
		N	6	6	6
	TOTB03	Correlation Coefficient	1,000	-,161**	-,244**
		Sig. (2-tailed)	.	,005	,000
		N	187	187	187
AirTemp03	Correlation Coefficient	-,161**	1,000	,693**	
	Sig. (2-tailed)	,005	.	,000	
	N	187	365	365	
WaterTemp03	Correlation Coefficient	-,244**	,693**	1,000	
	Sig. (2-tailed)	,000	,000	.	
	N	187	365	365	
** . Correlation is significant at the 0.01 level (2-tailed).					
* . Correlation is significant at the 0.05 level (2-tailed).					

Results for the year 2004

Correlations					
			TOTB04	AirTemp04	WaterTemp04
Kendall's tau_b	CB04	Correlation Coefficient	,602**	-,008	-,037
		Sig. (2-tailed)	,000	,917	,614
		N	123	123	123
	CPB04	Correlation Coefficient	,407**	,180	,180
		Sig. (2-tailed)	,005	,157	,157
		N	43	43	43
	JB04	Correlation Coefficient	,250	,121	,137
		Sig. (2-tailed)	,142	,417	,357
		N	32	32	32
	LB04	Correlation Coefficient	,156	-,182	-,132
		Sig. (2-tailed)	,355	,229	,385
		N	31	31	31
	POB04	Correlation Coefficient	,102	-,220	-,220
		Sig. (2-tailed)	,735	,414	,414
		N	11	11	11
	OB04	Correlation Coefficient	.	.	.
		Sig. (2-tailed)	.	.	.
		N	9	9	9
	TOTB04	Correlation Coefficient	1,000	-,076	-,075
		Sig. (2-tailed)	.	,184	,190
		N	192	192	192
	AirTemp04	Correlation Coefficient	-,076	1,000	,669**
		Sig. (2-tailed)	,184	.	,000
		N	192	366	366
WaterTemp04	Correlation Coefficient	-,075	,669**	1,000	
	Sig. (2-tailed)	,190	,000	.	
	N	192	366	366	

** . Correlation is significant at the 0.01 level (2-tailed).

Results for the year 2005

Correlations					
			TOTB05	AirTemp05	WaterTemp05
Kendall's tau_b	CB05	Correlation Coefficient	,502**	-,070	-,131
		Sig. (2-tailed)	,000	,438	,146
		N	83	83	83
	CPB05	Correlation Coefficient	,267	,009	-,027
		Sig. (2-tailed)	,090	,948	,845
		N	38	38	38
	JB05	Correlation Coefficient	,394*	-,069	-,179
		Sig. (2-tailed)	,026	,658	,255
		N	29	29	29
	LB05	Correlation Coefficient	.	.	.
		Sig. (2-tailed)	.	.	.
		N	21	21	21
	POB05	Correlation Coefficient	,280	,062	,062
		Sig. (2-tailed)	,183	,741	,741
		N	21	21	21
	OB05	Correlation Coefficient	.	.	.
		Sig. (2-tailed)	.	.	.
		N	13	13	13
	TOTB05	Correlation Coefficient	1,000	-,194**	-,185**
		Sig. (2-tailed)	.	,003	,004
		N	152	152	152
AirTemp05	Correlation Coefficient	-,194**	1,000	,688**	
	Sig. (2-tailed)	,003	.	,000	
	N	152	365	365	
WaterTemp05	Correlation Coefficient	-,185**	,688**	1,000	
	Sig. (2-tailed)	,004	,000	.	
	N	152	365	365	
** . Correlation is significant at the 0.01 level (2-tailed).					
* . Correlation is significant at the 0.05 level (2-tailed).					

Results for the year 2006

Correlations					
			TOTB06	AirTemp06	Watertemp06
Kendall's tau_b	CB06	Correlation Coefficient	,574**	-,135	-,094
		Sig. (2-tailed)	,000	,085	,250
		N	104	104	104
	CPB06	Correlation Coefficient	,296*	,104	,089
		Sig. (2-tailed)	,018	,350	,428
		N	56	56	56
	JB06	Correlation Coefficient	,405*	-,215	-,275
		Sig. (2-tailed)	,010	,138	,065
		N	33	33	33
	LB06	Correlation Coefficient	,330*	,032	,033
		Sig. (2-tailed)	,042	,826	,824
		N	34	34	34
	POB06	Correlation Coefficient	,063	,108	,151
		Sig. (2-tailed)	,771	,584	,458
		N	19	19	19
	OB06	Correlation Coefficient	.	.	.
		Sig. (2-tailed)	.	.	.
		N	3	3	3
	TOTB06	Correlation Coefficient	1,000	-,089	-,088
		Sig. (2-tailed)	.	,123	,134
		N	182	182	182
AirTemp06	Correlation Coefficient	-,089	1,000	,685**	
	Sig. (2-tailed)	,123	.	,000	
	N	182	365	365	
Watertemp06	Correlation Coefficient	-,088	,685**	1,000	
	Sig. (2-tailed)	,134	,000	.	
	N	182	365	365	
**. Correlation is significant at the 0.01 level (2-tailed).					
*. Correlation is significant at the 0.05 level (2-tailed).					

Results for the year 2007

Correlations					
			TOTB07	AirTemp07	WaterTemp07
Kendall's tau_b	CB07	Correlation Coefficient	,541**	-,098	-,130
		Sig. (2-tailed)	,000	,301	,171
		N	71	71	71
	CPB07	Correlation Coefficient	,375**	,107	,086
		Sig. (2-tailed)	,004	,349	,448
		N	52	52	52
	JB07	Correlation Coefficient	,318	-,247	-,123
		Sig. (2-tailed)	,127	,186	,509
		N	21	21	21
	LB07	Correlation Coefficient	,219	-,354	-,306
		Sig. (2-tailed)	,362	,104	,159
		N	16	16	16
	POB07	Correlation Coefficient	,228	,000	-,054
		Sig. (2-tailed)	,243	1,000	,754
		N	24	24	24
	OB07	Correlation Coefficient	,513**	-,186	,000
		Sig. (2-tailed)	,002	,205	1,000
		N	33	33	33
	TOTB07	Correlation Coefficient	1,000	-,096	-,104
		Sig. (2-tailed)	.	,120	,093
		N	157	157	157
AirTemp07	Correlation Coefficient	-,096	1,000	,668**	
	Sig. (2-tailed)	,120	.	,000	
	N	157	365	365	
WaterTemp07	Correlation Coefficient	-,104	,668**	1,000	
	Sig. (2-tailed)	,093	,000	.	
	N	157	365	365	
**. Correlation is significant at the 0.01 level (2-tailed).					

Results for the year 2008

Correlations					
			TOTB08	AirTemp08	WaterTemp08
Kendall's tau_b	CB08	Correlation Coefficient	,514**	-,198*	-,195*
		Sig. (2-tailed)	,000	,028	,030
		N	84	84	84
	CPB08	Correlation Coefficient	,498**	-,206	-,169
		Sig. (2-tailed)	,000	,080	,152
		N	50	50	50
	JB08	Correlation Coefficient	.	.	.
		Sig. (2-tailed)	.	.	.
		N	19	19	19
	LB08	Correlation Coefficient	,252	,294	,137
		Sig. (2-tailed)	,264	,148	,500
		N	18	18	18
	POB08	Correlation Coefficient	,199	,169	,290
		Sig. (2-tailed)	,353	,378	,131
		N	20	20	20
	OB08	Correlation Coefficient	,331	-,424*	-,166
		Sig. (2-tailed)	,109	,021	,367
		N	21	21	21
	TOTB08	Correlation Coefficient	1,000	-,253**	-,241**
		Sig. (2-tailed)	.	,000	,000
		N	158	158	158
AirTemp08	Correlation Coefficient	-,253**	1,000	,627**	
	Sig. (2-tailed)	,000	.	,000	
	N	158	366	366	
WaterTemp08	Correlation Coefficient	-,241**	,627**	1,000	
	Sig. (2-tailed)	,000	,000	.	
	N	158	366	366	
** . Correlation is significant at the 0.01 level (2-tailed).					
* . Correlation is significant at the 0.05 level (2-tailed).					

Results for the year 2009

Correlations					
			TOTB09	AirTemp09	WaterTemp09
Kendall's tau_b	CB09	Correlation Coefficient	,549**	-,363*	-,533**
		Sig. (2-tailed)	,001	,011	,000
		N	33	33	33
	CPB09	Correlation Coefficient	.	.	.
		Sig. (2-tailed)	.	.	.
		N	16	16	16
	JB09	Correlation Coefficient	,251	-,111	-,268
		Sig. (2-tailed)	,363	,664	,306
		N	12	12	12
	LB09	Correlation Coefficient	.	.	.
		Sig. (2-tailed)	.	.	.
		N	4	4	4
	POB09	Correlation Coefficient	.	.	.
		Sig. (2-tailed)	.	.	.
		N	10	10	10
	OB09	Correlation Coefficient	,455**	,126	,021
		Sig. (2-tailed)	,004	,363	,882
		N	36	36	36
	TOTB09	Correlation Coefficient	1,000	-,169	-,246**
		Sig. (2-tailed)	.	,053	,006
		N	81	81	81
AirTemp09	Correlation Coefficient	-,169	1,000	,644**	
	Sig. (2-tailed)	,053	.	,000	
	N	81	150	150	
WaterTemp09	Correlation Coefficient	-,246**	,644**	1,000	
	Sig. (2-tailed)	,006	,000	.	
	N	81	150	150	
** . Correlation is significant at the 0.01 level (2-tailed).					
* . Correlation is significant at the 0.05 level (2-tailed).					

Results for all the years together

Correlations					
			TB	AirTemp	WaterTemp
Kendall's tau_b	CB	Correlation Coefficient	,590**	-,015	-,151**
		Sig. (2-tailed)	,000	,589	,000
		N	856	856	856
	CPB	Correlation Coefficient	,058	,001	,038
		Sig. (2-tailed)	,216	,985	,347
		N	399	399	399
	JB	Correlation Coefficient	-,029	-,101	,020
		Sig. (2-tailed)	,628	,056	,707
		N	240	240	240
	LB	Correlation Coefficient	,000	-,011	-,102
		Sig. (2-tailed)	,992	,853	,075
		N	202	202	202
	POB	Correlation Coefficient	,022	,102	-,020
		Sig. (2-tailed)	,781	,138	,768
		N	143	143	143
	OB	Correlation Coefficient	-,075	-,090	,168*
		Sig. (2-tailed)	,390	,231	,025
		N	118	118	118
	TB	Correlation Coefficient	1,000	-,030*	-,141**
		Sig. (2-tailed)	.	,030	,000
		N	3072	3072	3072
	Airtemp	Correlation Coefficient	-,030*	1,000	,009
		Sig. (2-tailed)	,030	.	,475
		N	3072	3072	3072
Watertemp	Correlation Coefficient	-,141**	,009	1,000	
	Sig. (2-tailed)	,000	,475	.	
	N	3072	3072	3072	
** . Correlation is significant at the 0.01 level (2-tailed).					
* . Correlation is significant at the 0.05 level (2-tailed).					

Example of elaboration of break data

circumferential	corrosion pit	Joint	longitudinal	Piece out of the pipe	other	TOTAL BREAKS	Date	Outdoor temp C	water temp
1						1	01/01/2001	-3,73143	3,6
1						1	02/01/2001	-4,24548	3,59784
2	1			1		4	03/01/2001	1,10754	3,26511
4			1	1		6	04/01/2001	2,64137	3,09337
1			1			2	05/01/2001	2,03254	3,0303
						0	06/01/2001	2,85631	3,01333
2						2	07/01/2001	3,93734	3,0303
2						2	08/01/2001	5,07483	3,0303
3						3	09/01/2001	4,91337	3,0303
3						3	10/01/2001	2,55057	3,11105
2		1				3	11/01/2001	-2,58944	3,03705
	1					1	12/01/2001	0,226363	3,03129
						0	13/01/2001	-0,99134	3,03801
						0	14/01/2001	-1,38089	3,10318
1						1	15/01/2001	-1,83897	3,22557
3						3	16/01/2001	0,772156	3,21006
1						1	17/01/2001	-1,15299	3,2365
	1	1				2	18/01/2001	-1,59662	3,2252
5						5	19/01/2001	-0,83064	3,22014
2						2	20/01/2001	-0,90771	3,22557
						0	21/01/2001	-0,58762	3,21498
3						3	22/01/2001	-0,15872	3,20795

1						1	23/01/2001	-0,32561	3,21226
1						1	24/01/2001	-0,31487	3,20836
1						1	25/01/2001	3,41873	3,11
1						1	26/01/2001	3,34052	3,07918
						0	27/01/2001	2,80413	3,07918
	1					1	28/01/2001	2,48443	3,07918
2	1					3	29/01/2001	0,920603	3,07918
1	1		1			3	30/01/2001	0,059669	3,07918
						0	31/01/2001	0,771824	3,39214